



Norwegian University of  
Science and Technology

# Ocean Colour and Phytoplankton Dynamics

An examination of the Forel-Ule scale in a  
modern context

**Julie Christine Towers Mynors**

Marine Coastal Development

Submission date: May 2017

Supervisor: Geir Johnsen, IBI

Co-supervisor: Zsolt Volent, SINTEF

Norwegian University of Science and Technology  
Department of Biology



## Contents

<b>ACKNOWLEDGEMENTS</b> .....	<b>III</b>
<b>ABSTRACT</b> .....	<b>IV</b>
<b>SAMMENDRAG</b> .....	<b>V</b>
<b>INTRODUCTION</b> .....	<b>1</b>
WHAT IS LIGHT.....	1
APPARENT OPTICAL PROPERTIES.....	3
INHERENT OPTICAL PROPERTIES.....	4
OCEAN COLOUR AS AN ESSENTIAL CLIMATE VARIABLE.....	6
AN INTRODUCTION TO THE SECCHI DISK AND FOREL-ULE SCALE.....	6
THE HUMAN EYE AS A SENSOR.....	7
PLANKTON DYNAMICS, PIGMENTS AND LIGHT CLIMATE.....	8
CASE 1 AND CASE 2 WATERS.....	10
CITIZEN SCIENCE FOR OCEAN COLOUR MEASUREMENTS.....	11
MEASURING <i>IN SITU</i> [CHL <i>A</i> ] BY FLUORESCENCE.....	12
USING PROXIES FOR PHYTOPLANKTON BIOMASS.....	12
THE AIMS OF THIS THESIS.....	13
<b>MATERIALS AND METHODS</b> .....	<b>15</b>
SAMPLING SITES.....	15
<i>Trondheim Biological Station (TBS)</i> .....	15
<i>Svalbard</i> .....	15
<i>Agdenes</i> .....	15
<i>Froan</i> .....	16
<i>South Pacific Ocean</i> .....	16
<i>Sandvika</i> .....	16
<i>Soneren</i> .....	16
FIELD MEASUREMENTS.....	19
<i>Secchi Depth and Forel-Ule Measurements</i> .....	19
<i>Water samples</i> .....	19
FIELD MEASUREMENTS USING INSTRUMENTS.....	20
<i>Rig construction</i> .....	20
<i>Irradiance, <math>E_{PAR}</math></i> .....	20
<i>Spectral irradiance, <math>E(\lambda)</math></i> .....	20

<i>Spectral transmission of Forel-Ule filters</i> .....	21
<i>Concentration measurements of Chl a, cDOM and TSM</i> .....	21
<i>Temperature, salinity and depth</i> .....	21
LAB WORK .....	22
<i>Filtration and fixation</i> .....	22
<i>Phytoplankton pigments</i> .....	23
<i>In vitro [Chl a]</i> .....	23
<i>Sedimentation and counting (Utermöhl method)</i> .....	23
DATA PROCESSING .....	24
<i>Calculating the attenuation coefficient</i> .....	24
<i>Calculating transmission of light through Forel-Ule filters</i> .....	25
<b>RESULTS</b> .....	<b>27</b>
SPRING BLOOM TIME SERIES OF AOPs AND IOPs.....	27
EVALUATION OF THE FOREL-ULE SCALE .....	33
EVALUATION OF THE USE OF THE FOREL-ULE SCALE FOR CITIZEN SCIENCE .....	40
<b>DISCUSSION</b> .....	<b>42</b>
SPRING BLOOM TIME SERIES OF AOP AND IOP.....	42
EVALUATING THE FOREL-ULE SCALE.....	44
EVALUATION OF THE USE OF THE FOREL-ULE SCALE FOR CITIZEN SCIENCE .....	47
<b>CONCLUSIONS AND FUTURE PERSPECTIVES</b> .....	<b>50</b>
<b>BIBLIOGRAPHY</b> .....	<b>52</b>
<b>APPENDIX 1</b> .....	<b>56</b>
CITCLOPS APP INSTRUCTIONS TAKEN FROM CITCLOPS.EU.....	56
EYEWATER INSTRUCTIONS TAKEN FROM THE APPLICATION .....	57
<i>Introduction movie</i> .....	57
<i>Home page of the app</i> .....	61
<i>How to use the app</i> .....	62
<b>APPENDIX 2</b> .....	<b>71</b>
SUMMARY OF FINAL MODEL USING [cDOM] AND BETA(700) AS PREDICTOR VARIABLES .....	71
SUMMARY OF MODEL USING ONLY [CHL A] AS A PREDICTOR VARIABLE .....	71

## Acknowledgements

Most of the work this master thesis is based on was conducted at Trondheim Biological Station, NTNU, under the supervision of Prof. Geir Johnsen at NTNU and Senior Research Scientist Zsolt Volent at Sintef. In addition, data came from the Kon-Tiki 2 expedition, Sintef's ENTiCE project, and the AB323 Light Climate and Primary Production in the Arctic course in May 2016.

I want to thank my supervisor Prof. Geir Johnsen for his endless optimism and enthusiasm throughout the project. I would also like to thank my supervisor Zsolt Volent for his patience and good humour, as well as his dedication to my understanding of the relevant concepts. I also wish to thank Matilde Skogen Chauton at Sintef for help with phytoplankton identification. I am also grateful to Kjersti Andresen, Øystein Leiknes, Sturla Haltbakk and Nicole Aberle-Malzahn for their patience with my questions and their willingness to help. I want to thank all the staff at Trondheim Biological Station for including me and making me feel welcome, and thereby making the two years I have spent here very enjoyable. I also wish to thank my fellow master students at Trondheim Biological Station for the great discussions, support and help they have given me.

I further wish to thank the Kon-Tiki 2 expedition for including my measurements in the ones conducted, and special thanks to Pedro De La Torre for conducting the measurements from the raft. I also wish to thank the ENTiCE project for including me in their project and conducting measurements for me on their cruise in June 2016. I also wish to thank all the participants of the AB 323 Light Climate and Primary Production in the Arctic for the data collected, which was used in this thesis.

Finally I wish to thank my friends and family for their unfailing support, help and patience. Special thanks go to Maria Mynors, John Kjekken and Liz Percival for their help and support during the final days of writing.

Cover image: A Secchi disk at half Secchi depth in four different water masses, with different colours.

## Abstract

The Forel-Ule scale as a method of determining ocean colour has been in use for over 100 years. Ocean colour is a result of inherent optical properties (IOP) in the water, including phytoplankton biomass, coloured dissolved organic matter and total suspended particulate matter. The Forel-Ule ocean colour scale (a 21 colour comparator scale for categorising ocean colour) was used in conjunction with modern optical instruments and methods to detect apparent optical properties (AOP) and IOP of seawater through a spring bloom period. Measurements were also done in order to evaluate the Forel-Ule scale for use in modern science, both as a tool for scientists, and for citizen science. The spring bloom period for which measurements were done was found to have two separate phytoplankton blooms of different phytoplankton compositions. The two blooms were found using all modern methods, but the Forel-Ule numbers and Secchi depth showed no such trend. However, a way of isolating the part of the Forel-Ule number not determined by the Secchi depth was found by subtracting the Forel-Ule number and Secchi depth measured from the maximum Forel-Ule number, 21. This factor, named the Forel-Ule No Secchi (FUNS) factor, showed the two blooms found during the spring bloom period, indicating that it might be determined by the concentration of Chlorophyll *a* to a greater degree than is the Forel-Ule number. The Forel-Ule scale is found to be the most useful in the interpretation of large-scale observations of ocean colour, for example from remote sensing, for creating maps of oceanographic information, and in connecting historical ocean colour data with present-day ocean colour measurements. However, the scale was found to be of less use in citizen science due to variation in results recorded by different individuals. In addition there were large differences between results when using the plastic Forel-Ule scale and the smartphone applications intended for use in citizen science.

## Sammendrag

Forel-Ule-skalaen som metode for bestemmelse av havfarge har vært i bruk i over 100 år. Havfarge er et resultat av iboende optiske komponenter i vannet, inkludert fytoplanktonbiomasse, farget oppløst organisk materiale og totalt suspendert partikulært materiale. Forel-Ule-skalaen (en sammenligningsskala med 21 farger for å kategorisere havfarge) ble brukt sammen med moderne optiske instrumenter og metoder for å måle synlige og iboende optiske egenskaper av vannet i en våroppblomstringsperiode. Målinger ble også gjort for å kunne vurdere Forel-Ule-skalaen for bruk i moderne vitenskap, både som et verktøy for forskere og for borgervitenskap. Våroppblomstringsperioden som ble målt ble funnet å ha to separate fytoplankton-oppløst stringer av ulike sammensetninger. De to oppløst stringene ble funnet av alle moderne metoder, men Forel-Ule tallene viste ingen slik trend. Imidlertid ble en måte å isolere delen av Forel-Ule-nummeret ikke bestemt av Secchi-dybden funnet ved å trekke Forel-Ule tall og Secchi dybde fra det høyeste Forel-Ule tallet, 21. Denne faktoren, kalt Forel-Ule Ingen Secchi (FUNS) faktoren, viste de to oppløst stringene som ble funnet under våroppblomstringsperioden, og dette indikerer at faktoren muligens er bestemt av konsentrasjonen av Klorofyll *a* i større grad enn Forel-Ule tallet er. Forel-Ule-skalaen ble funnet å være mest nyttig i forståelsen av storskala observasjoner av havfarge, for eksempel fra satelittsensorer, til å lage kart over oseanografisk informasjon, og til å forbinde historiske havfargedata med dagens havfargemålinger. Bruken av Forel-Ule skalaen i borgervitenskap ble derimot funnet å være mindre nyttig på grunn av variasjon i resultater registrert av forskjellige individer. I tillegg var det store forskjeller mellom Forel-Ule-skalaen i plast og smarttelefonapplikasjonene beregnet for bruk i borgervitenskap.

## Introduction

The colour of the sea has fascinated people for a long time. The waves may twinkle like gilded emeralds, but can the colour of the water tell us anything about the abundance of species of microscopic phytoplankton just below the waves? This information would help enhance our understanding of the phytoplankton biodiversity and biomass throughout the year on a local to global scale.

In this thesis, I will attempt to answer parts of the question posed above, mainly by evaluating a colour comparator scale that has been in use for more than a hundred years, the Forel-Ule scale of ocean colour. The scale has 21 colours, ranging from deep blue via green to brown, and was created in the late 1800s by François-Alphonse Forel (blue to green) and Willi Ule (green to brown) (Forel 1890; Ule 1892). It is used to categorise ocean colour, and will in this thesis be compared to modern optical sensors (underwater spectroradiometer and fluorescence- and backscattering sensor) and methods (HPLC and light microscopy) to identify inherent and apparent optical properties of water, especially phytoplankton biomass.

To understand the optical properties of water, we first need a general understanding of the light climate, consisting of irradiance, spectral irradiance, and day length.

## What is light

Light is electromagnetic radiation that can be classified into wavelengths, measured in nanometers (nm) (Sakshaug et al. 2009b). The electromagnetic radiation from the Sun includes radio waves, infrared radiation, and ultraviolet radiation among many other types (Figure 1). The visible spectrum of light is defined to be in the range 400-700 nm, which are the wavelengths generally visible to the human eye, and that is also the energy window for photosynthesis, known as Photosynthetically Available Radiation (PAR) (Sakshaug et al. 2009b).

The light from the Sun that reaches the ground does not have equal intensity across all wavelengths and is altered by solar elevation, clouds, humidity and aerosols (Sakshaug et al. 2009b). It has approximately equal intensity across the visible spectrum, but most ultraviolet (UV, <400 nm) light and some infrared radiation (IR, >700), also known as heat, have been



removed by both the gases in the outer parts of the Sun and the Earth's atmosphere (Sakshaug et al. 2009b).

Irradiance is the sum of radiation from all directions hitting a surface, such as the sea surface (Sakshaug et al. 2009b). It is measured using a flat and horizontal, or cosine corrected, light collector taking in light from a 180 degree angle above it, i.e. half a sphere (Sakshaug et al. 2009b). Irradiance is not to be confused with radiance, which measures a much smaller angle of incident radiation (Jerlov 1976).

When the incident sunlight is at a more oblique angle, the incident radiation is spread over a larger surface area, meaning each patch of sea or land receives less of the total radiation than if the incident sunlight was at 90 degrees (Sakshaug et al. 2009b). This is an important factor in the irradiation received in the higher latitudes of the Subarctic and Arctic, as the angle of incident sunlight is more oblique further North.

As the light hits the surface of the ocean, it may be reflected or absorbed. If the incident angle of the light is close to 90 degrees, the chances of absorption go up dramatically (Kirk 1994). This means that if the sun angle is low, a large portion of the incident radiation would generally be reflected, but the portion of absorbed light could increase if there were waves, shifting the incident angle on the surface of the water towards 90 degrees (Kirk 1994).

Light is known to behave both as a particle and a wave, and the light particle, or photon, can be thought of as a 'wave packet' (Sakshaug et al. 2009b). As one photon, or quantum, is needed to activate one light harvesting complex in a photosynthetic organism, the incident irradiance for a wave band is usually measured by the unit quanta per area (eg.  $\text{m}^{-2}$ ) per time (eg.  $\text{s}^{-1}$ ), usually  $\mu\text{mol quanta m}^{-2} \text{s}^{-1}$  (Sakshaug et al. 2009b). For biological purposes, the incident irradiance is often measured for PAR and denoted  $E_{\text{PAR}}$  (Sakshaug et al. 2009b). Light climate is defined as the irradiance ( $E$ ,  $\mu\text{mol quanta m}^{-2} \text{s}^{-1}$ ), the spectral irradiance ( $E(\lambda)$ ,  $\mu\text{mol quanta m}^{-2} \text{s}^{-1} \lambda^{-1}$ ) and the day length ( $h$ ) (Sakshaug et al. 2009b), and is important to phytoplankton dynamics.

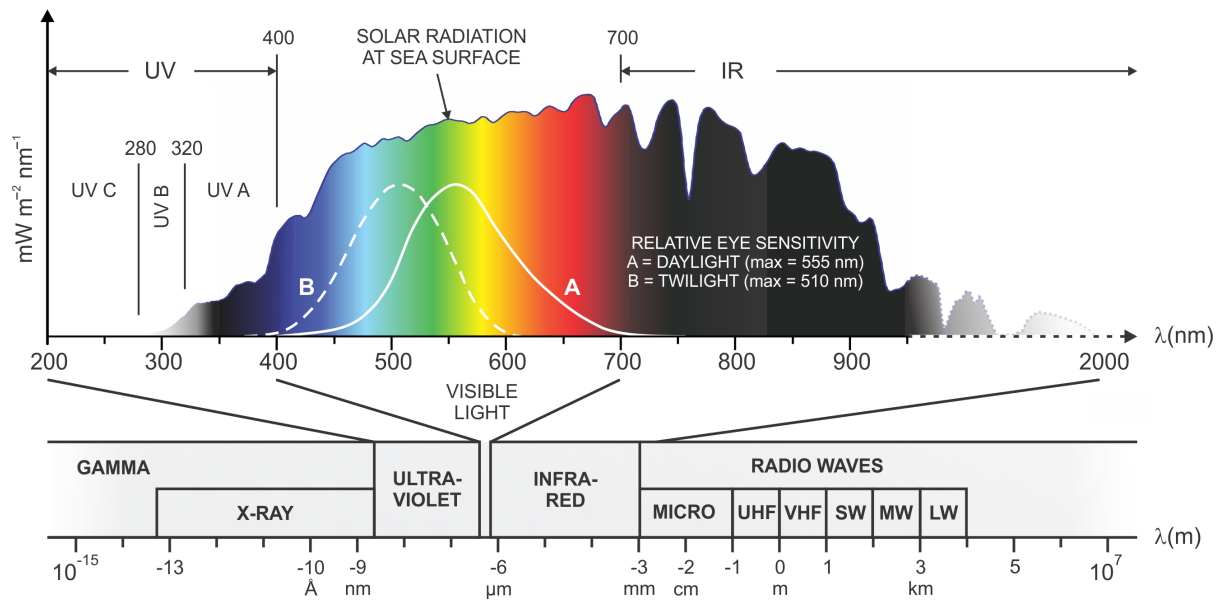


**Figure 1: The solar spectrum at the sea surface. The relative sensitivity of the human eye in daylight and twilight are also shown. Figure from Sakshaug et al. (2009b).**

### Apparent optical properties

Once absorbed or passed through the air-water interface, the light will be scattered and absorbed by the substances in the water and the water itself. Apparent optical properties (AOP) of water are the optical properties of water as measured using only sunlight as a light source (Preisendorfer 1976). These measurements are dependent on the light from the sun, the weather, sun angle, waves, and the substances in the water (Sakshaug et al. 2009b). These factors can sometimes result in the ocean looking grey from reflected and scattered light, or mirror-like, reflecting the sky and surrounding objects.

Apparent optical properties are generally easy to measure but hard to interpret, as no light source is needed beyond the natural light present (Sakshaug et al. 2009b). In the case of some of the AOP measurements done in this master, the only things needed were a few simple devices and a human to look and record. Along with irradiance and spectral irradiance at different depths, as well as many other types of measurements, ocean clarity and ocean colour, as measured by Secchi depth and Forel-Ule number for example, are apparent optical properties of the water (Sakshaug et al. 2009b).

The reason that AOPs are hard to interpret is the convoluted nature of the factors involved (Sakshaug et al. 2009b). It is hard to find out which single factor might be responsible for a

change in a measurement of an apparent optical property, such as differences in colour or intensity.

Attenuation of light in the water column is due to the absorption and scattering of light by water and the substances in it (Sakshaug et al. 2009b). The diffuse attenuation coefficient,  $K$ , is calculated using Equation 2, 3, 4 or 5 shown in Materials and Methods, depending on what measure of attenuation is the starting point (Watson and Zielinski 2013).

### **Inherent optical properties**

Inherent optical properties are the optical properties of the water itself with any substances in it (Preisendorfer 1976). Inherent optical properties are measured using instruments with their own light source, and other light must be controlled for or taken into account when analysing the data (Sathyendranath 2000). The substances in the water includes pure water, and the categories coloured Dissolved Organic Matter (cDOM), Total Suspended Matter (TSM), and phytoplankton pigments (Sakshaug et al. 2009b), such as Chlorophyll *a* (Chl *a*) as well as other chlorophylls, carotenoids and phycobiliproteins (Roy et al. 2011).

Pure water absorbs red and green light, and scatters blue light (Sakshaug et al. 2009b). It therefore appears blue to the eye. When you descend into the water column, the red light is heavily attenuated, leaving green and blue (Sakshaug et al. 2009b). The green light then disappears, leaving only the blue light to penetrate deep into the water. This is shown in Figure 2, which also shows that in fjord water, blue light is also attenuated, due to the presence of cDOM, making it appear green (Sakshaug et al. 2009b).

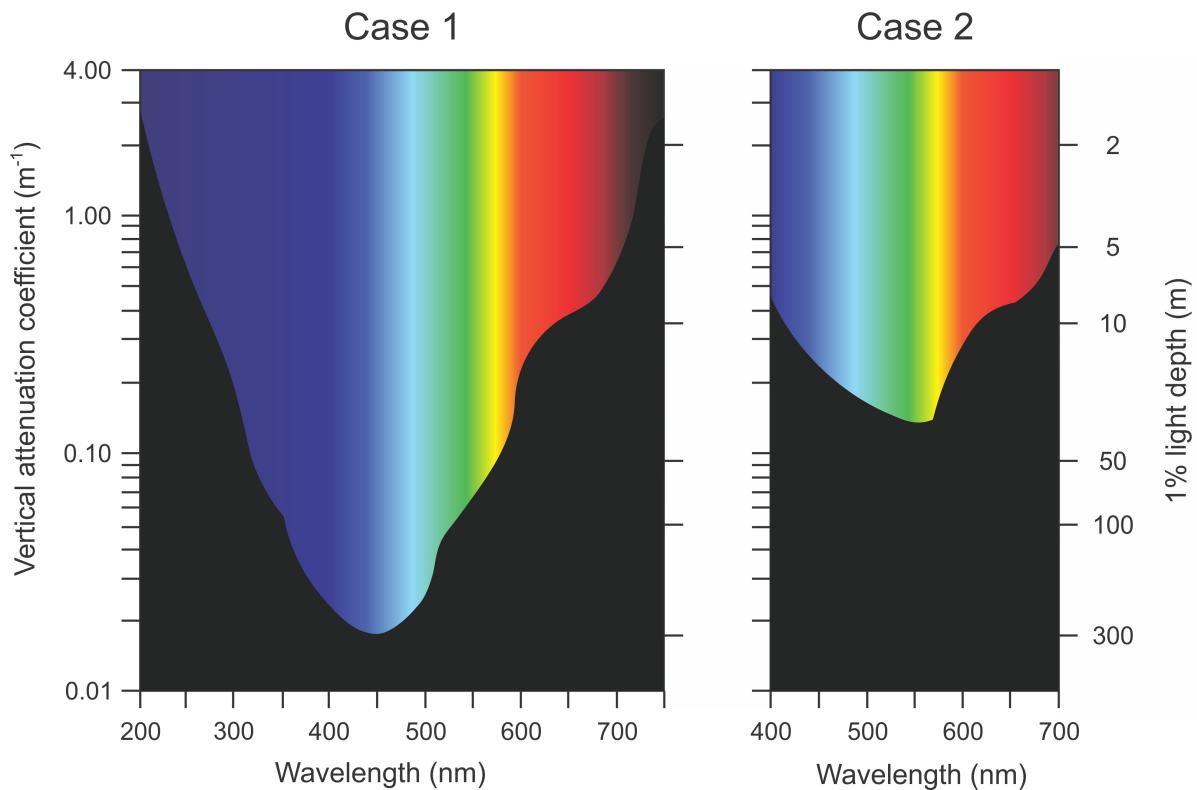


**Figure 2: Vertical diffuse attenuation coefficients for different wavelengths for clear oceanic water and fjord water. In fjord water cDOM causes attenuation of blue wavelengths, causing green light to be the deepest penetrating wavelength. Figure from Sakshaug et al. (2009b)**

cDOM is a collection of coloured molecules that are the result of the decomposition of organisms (Kirk 1994). The sources of cDOM in marine environments are from river run-off containing decayed plant material or soil, or from marine sources such as the decomposition of phyto- and zooplankton and from kelp forests, that release large amounts of polyphenols (Kirk 1994; Valle 2014). Collectively, these appear yellow-brown at high concentrations (Johnsen et al. 2009). At low concentrations of cDOM, the originally blue colour of the water appears greenish (Johnsen et al. 2009).

TSM are small particles such as silt, minerals and colloids, which are suspended in the water column and mainly come from river run-off (Sakshaug et al. 2009b). This includes any suspended matter, including biological matter such as phytoplankton and marine snow (Sakshaug et al. 2009b). At high concentrations of TSM, the water appears grey or greyish-brown. Some inorganic suspended material may be organic in origin, such as the chalk plates, or coccoliths, surrounding cells of the bloom-forming prymnesiophycean *Emiliania huxleyi* (Johnsen et al. 2009). These can be traced by ocean colour detecting satellites since the

coccoliths heavily scatter light, making the seawater appear turquoise (Johnsen et al. 2009). This is the same effect as that of glacial river run-off with mineral particles of inorganic origin (Johnsen et al. 2009).

Chl *a* is the most common phytoplankton pigment, and exists in most known autotrophic phytoplankton (Jeffrey et al. 2011). It is also the most measured pigment, and is used as a proxy for phytoplankton biomass. Chl *a* is olive green when at high concentrations (Jeffrey et al. 2011). Fucoxanthin and Peridinin, two other common light harvesting pigments (LHP), make phytoplankton appear brown at high concentrations (Jeffrey et al. 2011).

Inherent optical properties are hard to measure properly due to the spectral properties of the light source used, and the extra battery use due of the light source. However, measurements of inherent optical properties are easy to interpret due to all factors being known, and instruments or software often provide concentrations directly, which, if the instrument is calibrated correctly, can be accurate (Johnsen et al. 2009).

### **Ocean colour as an essential climate variable**

Along with other key environmental variables, such as salinity and temperature, ocean colour has been chosen as an Essential Climate Variable by the Global Climate Observing System, GCOS, to support the work of the Intergovernmental Panel on Climate Change (IPCC) and the United Nations Framework Convention on Climate Change (UNFCCC) (Mason and Reading 2005). This variable is mainly considered important due to the information gathered from remote sensing in conjunction with historical ocean colour observations (Mason and Reading 2005). The information gathered by remote sensing may be supported by *in situ* measurements of ocean colour (Mason and Reading 2005). Ocean colour provides estimates for primary production, cDOM concentrations, and the distributions of certain easy-to-monitor phytoplankton, such as *Emiliana huxleyi*, which is easy to monitor due to the scattering of light by the coccoliths in the shell of this species (Johnsen et al. 2009).

### **An introduction to the Secchi disk and Forel-Ule scale**

The colour of the sea was a useful observation for sailors already from the time of Hudson in the early 17<sup>th</sup> century to avoid shallow regions and submerged parts of icebergs (Wernand 2011). It was therefore important to know what colour the ocean had to the eye at different depths. Many other people, for example Otto von Kotzebue and Captain Bérard, had lowered

things into the ocean to test the transparency of the water (Cadée 1996) to satisfy curiosity and aid in understanding of the ocean before Father Angelo Secchi did tests in 1865 to refine the method and define a good universal method for this measurement (Wernand 2011). This was done to find an explanation for the transparency and colouration the ocean (Wernand 2011). Circular white disks with a weight to keep the disk horizontal as it was lowered became known as Secchi disks (Wernand 2011). The Secchi disk is in its essence still in use today (Wernand 2011).

It was still unclear how to categorize the colour of the sea, and the reasons for the blue colour of the open ocean were still under discussion (Wernand 2011). This question was finally settled by Chandrasekhara Venkata Raman, who found that the blue colour of the sea was due to the scattering of blue light by pure water (Raman 1922). To categorize the colour of the sea, colour comparator scales were created (Wernand 2011). The first standard for this was presented by François-Alphonse Forel in 1887 (Forel 1890). It covers the blue to the green region, and is a mix of solutions of copper sulphate and potassium chromate (Wernand 2011). The scale was extended by Willi Ule in 1892 towards the brownish colours, adding cobalt sulphate (Ule 1892). The scale then became known as the Forel-Ule scale, with 21 different coloured solutions in glass tubes (Wernand 2011). The scale has been in use since then, with hundreds of thousands of measurements having been made (Wernand, 2011). The modern version of the scale consists of plastic filters instead of glass vials, but is built in the same way, with a white background behind half the filter or vial, and a comparator opening behind the other half (Wernand 2011).

### **The human eye as a sensor**

The retina of the human eye has two types of photoreceptive sensory cells, rods that are sensitive to low light but not colour, and cones that are sensitive to colour at high light levels (Wernand 2011). The cones contain one of three photo-pigments, and are sensitive to the red, green or blue part of the visible spectrum (Wernand 2011). Colour blindness occurs when there are anomalies in cones or a type of cone is missing altogether (Gegenfurtner and Sharpe 2001). Even in people who are not colour blind, colour perception varies, and this indicates the fallibility of the human eye as a sensor (Gegenfurtner and Sharpe 2001).

The human eye is sensitive to light from 380 nm to 780 nm, though 400-700 nm is generally considered to be the visible spectrum, coinciding with the PAR region (Sakshaug et al.

2009b). The maximum sensitivity of the human eye is at 555 nm in daylight, and 510 nm in twilight (Sakshaug et al. 2009b) (Figure 1).

It is not enough to only look at the biological entity of the human eye when considering its use as a sensor (Hubel 1963). Interpretation by the brain always plays a role in how we perceive the world around us (Hubel 1963). We are good at understanding what we would term the true colour of something even when light with different spectral composition is shining on it, such as at sunset (Foster et al. 1997). This can be compared to the white balance function in cameras, which try to approximate human vision using three sensors, sensitive to red, green and blue (RGB colours) (Sencar and Memon 2013). Different total intensities of the same spectral signature, with the same relative intensities of each wavelength, look like different colours to us, another indication that the human eye is not a good qualitative or quantitative light sensor (Roaf 1927).

### **Plankton dynamics, pigments and light climate**

Light climate, defined as the irradiance ( $E$ ,  $\mu\text{mol quanta m}^{-2} \text{s}^{-1}$ ), the spectral irradiance ( $E(\lambda)$ ,  $\mu\text{mol quanta m}^{-2} \text{s}^{-1} \lambda^{-1}$ ) and the day length ( $h$ ) (Sakshaug et al. 2009b), is an important factor for phytoplankton dynamics (Sakshaug et al. 2009a). These variables vary with latitude and the local biotic and abiotic environment. The day length increases day by day during a spring bloom period along the Norwegian coast, and the total light received per day seems to affect the start time of the spring bloom. The irradiance can vary with incident light angle and cloud cover, and in Trondheim, where most measurements were done, the maximum  $E_{\text{PAR}}$  is about  $1500 \mu\text{mol quanta m}^{-2} \text{s}^{-1}$  in midsummer, and about  $50 \mu\text{mol quanta m}^{-2} \text{s}^{-1}$  in midwinter (Valle 2014). The spectral irradiance found at any point in the ocean depends on the optically active substances of the water and the depth at which the measurement is done, as well as the spectral properties of the incident light (Sakshaug et al. 2009b).

Different phytoplankton have different suites of pigments, both light harvesting and photo-protective (Jeffrey et al. 2011). The light harvesting pigments (LHP) enable phytoplankton to utilise different parts of the visual spectrum (Roy et al. 2011). At different spectral light climates, this gives some groups an advantage, as they can make use of parts of the spectrum that the other types of phytoplankton do not (Sakshaug et al. 2009a). Major LHPs are Chlorophylls  $a$ ,  $b$ ,  $c_1$ ,  $c_2$  and  $c_3$ , Fucoxanthin, Peridinin, and Phycobilins (Jeffrey et al. 2011).

The photo-protective carotenoids, PPC, affect the colour of phytoplankton cells, and therefore the optical properties of the water, as well as giving an indication of the physiological and light protective state of the phytoplankton at the time of sampling (Roy et al. 2011). The phytoplankton pigments found in a water sample can also indicate the physiological state of the phytoplankton assemblage (Roy et al. 2011). If the phytoplankton have more than enough light, they may be high light acclimated, changing their pigments concentrations and ratios accordingly, increasing the amount of PPC and reducing the LHP such as Chl *a* (Roy et al. 2011). If the bloom is in a post-bloom phase, there may be a larger portion of decomposed pigments, for example degradation products of Chl *a*, such as Chlorophyllide *a*, Phaeophytin *a* and Phaeophorbide *a* (Roy et al. 2011).

As different groups of phytoplankton have different combinations of pigments, extracting and identifying pigments from a water sample can be used for taxonomic purposes (Roy et al. 2011). Some pigments, like Peridinin, only occur in dinoflagellates, and can therefore be used as an indicator that there are dinoflagellates present in the water if this pigment is found (Roy et al. 2011). The pigments, being coloured substances, also directly affect the ocean colour, and the colour of a concentrated bloom of one type of phytoplankton differs from another, see Figure 3 (Sakshaug et al. 2009a).

Phytoplankton need light and nutrients to survive. Nutrients can be supplied by river run-off, upwelling of nutrient rich water, or decomposition and mixing during the winter months (Sakshaug et al. 2009a). Enough light for survival relies on the mixing of the upper layer carrying the phytoplankton into the necessary light for long enough to enable the phytoplankton to survive the periods where there is too little light (Sverdrup 1953). If the phytoplankton sink out of the mixed layer, they will die from low light exposure. If the mixed layer is too deep, the phytoplankton will not survive the period spent in darkness (Sverdrup 1953). If the water is too turbid, the acceptable mixing depth to facilitate phytoplankton growth may be too shallow, and growth will not occur.

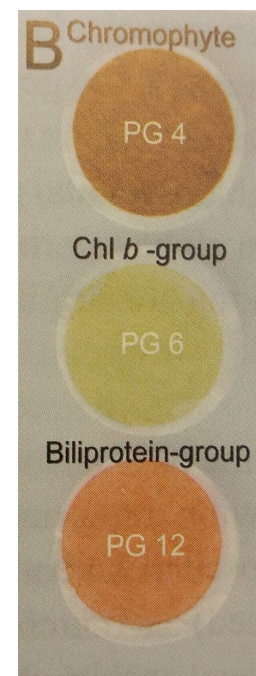


**Figure 3: The colour of different pigment groups as they appear on filters, when highly concentrated. Figure from Sakshaug et al. (2009a).**



The light climate drastically changes as a function of depth. The red light disappears first, and as a result this makes it unfeasible to utilise red light in energy production for phytoplankton (Sakshaug et al. 2009b). Where there are large amounts of phytoplankton, the wavelength bands useful to phytoplankton disappear quickly going down through the photic zone of the ocean (Sakshaug et al. 2009b). There are some algae that utilise the light found at greater depths, for example red algae (Karleskint et al. 2012). These algae, and some phytoplankton, have phycobiliproteins facilitating absorption and utilisation of blue and blue-green light (Roy et al. 2011). In the Trondheimsfjord, it has generally been found that spring blooms are dominated by diatoms, while dinoflagellates may dominate later blooms (Sakshaug 1972).

### **Case 1 and Case 2 waters**

Water masses have been divided into two main optical classes, Case 1 and Case 2 waters (Preisendorfer 1976; Sathyendranath 2000). Case 1 waters are water masses deemed optically simple, with only the water itself and the amount of phytoplankton determining the optics of the water, both the colour and the transparency (Sathyendranath 2000). This is usually found in the open ocean (Sakshaug et al. 2009b).

Case 2 waters are water masses deemed optically complex (Preisendorfer 1976). The optics in Case 2 waters are determined by a combination of the colour of the water itself, the concentration of cDOM, the amount of TSM, and the amount of phytoplankton (Sathyendranath 2000) (Figure 4). Case 2 waters are usually found closer to land than Case 1 waters, in waters affected by runoff (Sakshaug et al. 2009b).

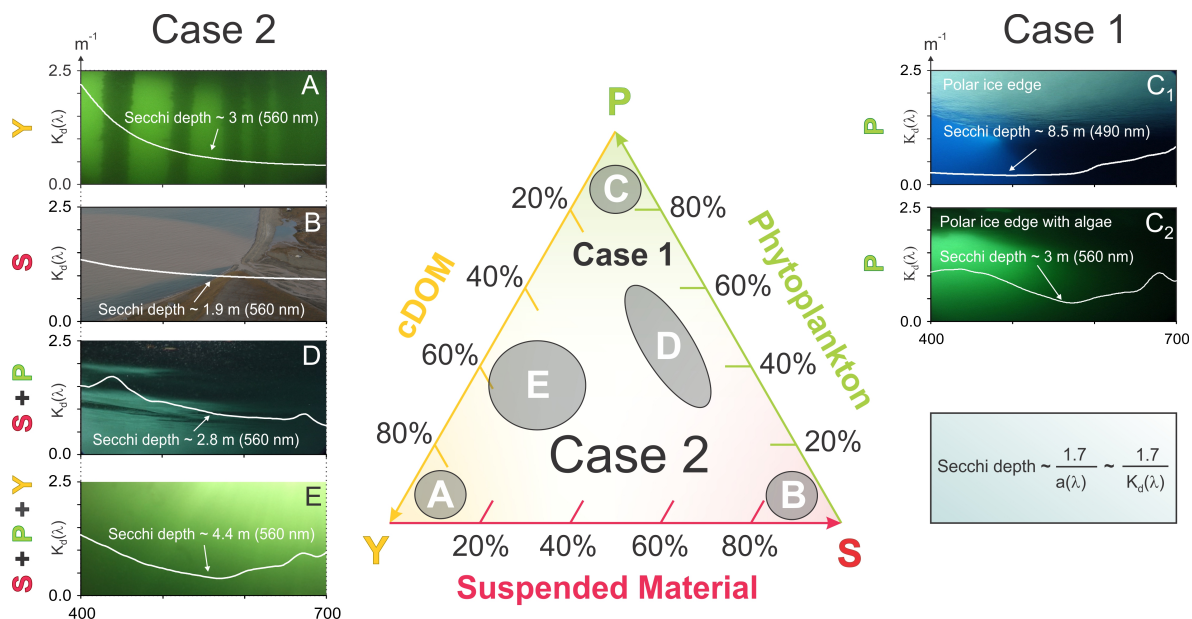


**Figure 4: The optical relationship between Case 1 and Case 2 waters, showing the optical components of seawater, phytoplankton (P, [Chl *a*]), cDOM (denoted Y in this figure), and suspended matter (denoted S in this figure). The pictures, corresponding to A-E, show different compositions of these components, together with the spectral attenuation and Secchi depth found for each instance. Figure from Johnsen et al. (2009)**

### Citizen science for Ocean Colour measurements

Citizen science projects involves members of the general public in the collection and analysis of data to answer questions about the natural world (Silvertown 2009). Through the use of the Forel-Ule applications (apps) developed by Maris based on a concept from the Netherlands Institute for Sea Research (NIOZ), people can become engaged in citizen science to record Forel-Ule values at a greater spatial and temporal distribution than that which is possible to achieve by scientists (Citclops 2014; MARIS and Citclops 2016).

Citizen science projects have a history of more than 100 years (Silvertown 2009). They usually engage hobby naturalists in collecting observations of organisms and therefore their distribution (Silvertown 2009). The longest-running and earliest citizen science project is the Christmas Bird Count in the US, which started in 1900 (Silvertown 2009). The data collected through citizen science have been very useful to science as a way of collecting large volumes of field data (Silvertown 2009). The wide availability of technology, Internet, and especially smartphones, facilitates citizen science to a large degree today, as it assists both recruiting and data collection (Silvertown 2009).

If citizen science can be used to educate people on the processes of science and connect knowledge to the process of creating said knowledge, this could help citizens engage with and trust science to a greater degree. However, most of the volunteers in citizen science projects are already science-positive and affluent (Martin 2017). This might be because most projects ask for volunteers to come to them, instead of reaching out to the community to conduct science on their premises (Martin 2017). The recruitment of people who are not that interested in science, and mostly feel that they can't understand it, is small (Martin 2017). The imagined positive effect of citizen science, increasing the number of science-positive people who will look to science for answers to problems, therefore looks to be lower than expected (Martin 2017).

### **Measuring *in situ* [Chl *a*] by fluorescence**

Fluorescence is the process in which a molecule absorbs light at one wavelength and emits light at a longer wavelength. The absorbed light excites an electron in the molecule to a higher unstable energy state and as the electron returns to a lower energy state, the excess energy is released as heat and visible light that has its emission peak at 685 nm (deep red by human eye) for phytoplankton *in vivo* (Suggett et al. 2010).

The concentrations of substances in water are often measured using fluorescence. In this thesis, *in situ* measurements of Chl *a* and cDOM are done using this method, where light is emitted to excite the molecule, and the light emitted back from the molecule is measured at a 90 degree angle relative to the excitation light to avoid the detection of stray light from the light source.

There are several things affecting measurements of the amount of Chl *a* in live cells using fluorescence. At high light, the pH in the thylakoid lumen is lowered, and this leads to lower fluorescence emitted from the cells and is mainly pH and PPC dependent (Brunet et al. 2011). The light source also needs to be at a high enough intensity to fully saturate the photosystems (PSI and PSII), which may not always be the case (Suggett et al. 2010).

### **Using proxies for phytoplankton biomass**

The amount of organically bound carbon present, or particulate organic carbon (POC) is a generally accepted and accurate measure of biomass (Johnsen et al. 2011). It is, however, affected by POC from bacteria (Simon et al. 1990). The relation of this measurement to the

proxies used is not always linear. This introduces complications, as other measurements of biomass are often easier to measure, but can be inaccurate (Johnsen et al. 2011).

Chl *a* concentration has long been used as a proxy for phytoplankton biomass, although the ratio of Chl *a* to carbon is in no way constant from organism to organism and is also heavily affected by photo-acclimation (Johnsen and Sakshaug 2007). Phytoplankton adjust the amount of Chl *a* in their cells according to the amount of light they are receiving, as well as regulating thylakoid stacking (Falkowski and Raven 2007). This is done over generations, equipping future daughter cells with more LHP if the cell has experienced low light conditions, and less LHP if the mother cell has experienced high light in its lifetime (Brunet et al. 2011).

Biovolume is also used as a proxy for biomass (Karlson et al. 2010). This is possible to estimate using measurements of the organisms and simple geometric formulas to calculate volume (Karlson et al. 2010). Wet or dry weight is often used for larger organisms, but is more demanding to use on plankton (Karlson et al. 2010).

Cell numbers or concentrations have also been used to indicate phytoplankton biomass (Karlson et al. 2010). Pure cell counts with no biovolume estimation are often an underrepresentation of the biomass present in the water (Karlson et al. 2010).. Counting using a microscope also means that there is a lower limit of cell size possible to see and therefore count (Karlson et al. 2010). There are usually photosynthetic organisms smaller than this limit, and these therefore get left out of the counts (Karlson et al. 2010).

Remote sensing of ocean colour, as [Chl *a*], has been used for approximation of phytoplankton biomass in recent years (Johnsen et al. 2009). This relies on satellite pictures of the sea surface, therefore missing out on any deeper blooms, and is measured using wavebands, for example a band centred at 443 nm to observe the Chl *a* absorption maximum (Johnsen et al. 2009). The estimation of biomass using ocean colour as observed by humans is not widely used in the present day.

### **The aims of this thesis**

Light climate is important to the primary production in the sea, and it is an important ecological factor that affects the whole ecosystem. It is therefore important to have a good

way to measure this. As technology has advanced, the instruments usually used for such measurements have become more complicated to use, and more expensive. This limits the number of measurements it is possible to obtain. If a simple and inexpensive method such as the Forel-Ule method could be used to obtain information useful to biological sciences, the use of citizen science could lead to the number of *in situ* measurements dramatically increasing. This could support data collected in other ways by scientists, and create a more detailed picture of the ecosystem.

This thesis aims to evaluate the Forel-Ule scale in a modern context by comparing it to modern measurements of light climate and evaluating its usefulness in modern science. This is done by comparing Forel-Ule measurements to measurements from modern sensors and evaluating the accuracy and reliability of Forel-Ule measurements. The degree to which the Forel-Ule scale may be able to give information about the concentrations of optically active components of seawater is also evaluated.

## Materials and Methods

### Sampling sites

Several sampling sites were used throughout this thesis project, see map in Figure 5. Different types of measurements were done for each sampling site according to the available equipment, see Table 1. All samplings and measurements were carried out in 2016.

#### Trondheim Biological Station (TBS)

Trondheim biological station (TBS) is situated in Trondheim, along the Trondheimsfjord, close to the mouth of the river Nidelva (63.4408 °N, 10.3490 °E). The sampling and measurement place, the dock, has a depth of about 11 m, depending on the tide. It is in the inner part of the fjord, heavily affected by runoff. In addition to sampling and measuring frequently during the spring bloom period, from the 8<sup>th</sup> of March to the 8<sup>th</sup> of April, measurements were done on the 26<sup>th</sup> of April and the 17<sup>th</sup> of June. A Forel-Ule user test was conducted on the 26<sup>th</sup> of April, when 8 different people determined the Secchi depth and Forel-Ule number within a time window of one hour.

#### Svalbard

Sampling was done from polarcirkel boats, at depths over 15 m. Three measurements were made outside Bjørndalen (78.2356 °N, 15.2951 °E) on the 9<sup>th</sup>, 10<sup>th</sup> and 11<sup>th</sup> of May, and the last measurement was made outside Longyearbyen, in Adventsfjorden (78.2390 °N, 15.7136 °E) on the 13<sup>th</sup> of May. Both sites were close to river-mouths, but at the time of sampling, both river systems were frozen. The absence of a glacial sill at the entrance of the fjord system means that there is a high exchange between shelf and Atlantic waters (Kedra et al. 2015). As a result of the increased influx of warmer Atlantic water, the fjord has remained largely ice free the last couple of years (Hegseth and Tverberg 2013).

#### Agdenes

The measurements at Agdenes were conducted from the research vessel R/V Gunnerus, at 63.6149 °N, 9.7759 °E on the 18<sup>th</sup> of April and the 21<sup>st</sup> of April. The site is the deepest point in the fjord, and also close to the glacial sill of the Trondheimsfjord. There are a lot of currents in the area, both deep and shallow. The water is affected by runoff and by exchange with the coastal water.

### **Froan**

Froan is an archipelago outside the Trondheimsfjord. Two measurements were done there, at 63.9503 °N, 8.6686 °E (Station 1), and at 63.9382 °N, 8.6381 °E (Station 2). Both the measurements were conducted on the 7<sup>th</sup> of June. It is highly affected by tidal currents and coastal water. It is largely shallow, with some deep channels between islands. It is the object of study by the project ENTiCE, to which my master has been connected. The project seeks to increase the spatial resolution of a marine model of the area, gaining understanding of the effect of high tidal currents on the primary production, especially at other times than well documented bloom times.

### **South Pacific Ocean**

The Pacific Ocean is the largest ocean on the planet, at 165.25 million km<sup>2</sup> (Cotter et al.). An expedition in the spirit of Thor Heyerdahl's Kon-Tiki expedition set off in the autumn of 2015, named Kon-Tiki 2 (Kon-Tiki2 2015). There were two balsa-wood rafts that journeyed from Peru to Easter Island, and then planned to return to Chile, but were unsuccessful in this. During the return journey, three measurements of ocean colour were conducted using a Secchi disk and a Forel-Ule scale, as described here. The measurements were carried out at 27.4127 °S, 109.1835 °W (Measurement 1, on the 9<sup>th</sup> of January), 32.2057 °S, 113.4897 °W (Measurement 2, on the 25<sup>th</sup> of January), 36.5862 °S, 111.3938 °W (Measurement 3, on the 9<sup>th</sup> of February).

### **Sandvika**

Sandvika is a town in the inner parts of the Oslofjord. The sampling place was close to the mouth of the river Sandvikselva. It was also near a harbour and construction work along the sandy coast, and quite shallow. The measurements were taken from the bridge connecting Kaddettangen to Kalvøya (59.8859 °N, 10.5332 °E) on the 24<sup>th</sup> of June.

### **Soneren**

Soneren is a humous-rich inland lake fed by rivers and streams originating from bogs. It is used as a reservoir of a small power plant, and the water level is therefore artificially controlled. The lake is surrounded by farmed land and forest. It is a lake in the Drammenselva drainage basin in southeast Norway. The measurements were done at 60.0555 °N, 9.5648 °E on the 28<sup>th</sup> of July.

**Table 1: The equipment and methods used for each sampling site.**

<b>Place</b>	<b>Secchi and Forel-Ule</b>	<b>Cell counts</b>	<b>Pigment analyses</b>	<b>ECO- TRIPLET</b>	<b>E<sub>PAR</sub></b>	<b>E(<math>\lambda</math>)</b>	<b>CTD</b>	<b>Fluoro- meter</b>
<b>TBS</b>	x	x	x	x	x			x
<b>Agdenes</b>	x	x	x				x	
<b>Svalbard</b>	x	x	x	x	x	x		
<b>Froan</b>	x		x	x		x	x	
<b>Sandvika</b>	x	x						
<b>Soneren</b>	x	x						
<b>South Pacific Ocean</b>	x							



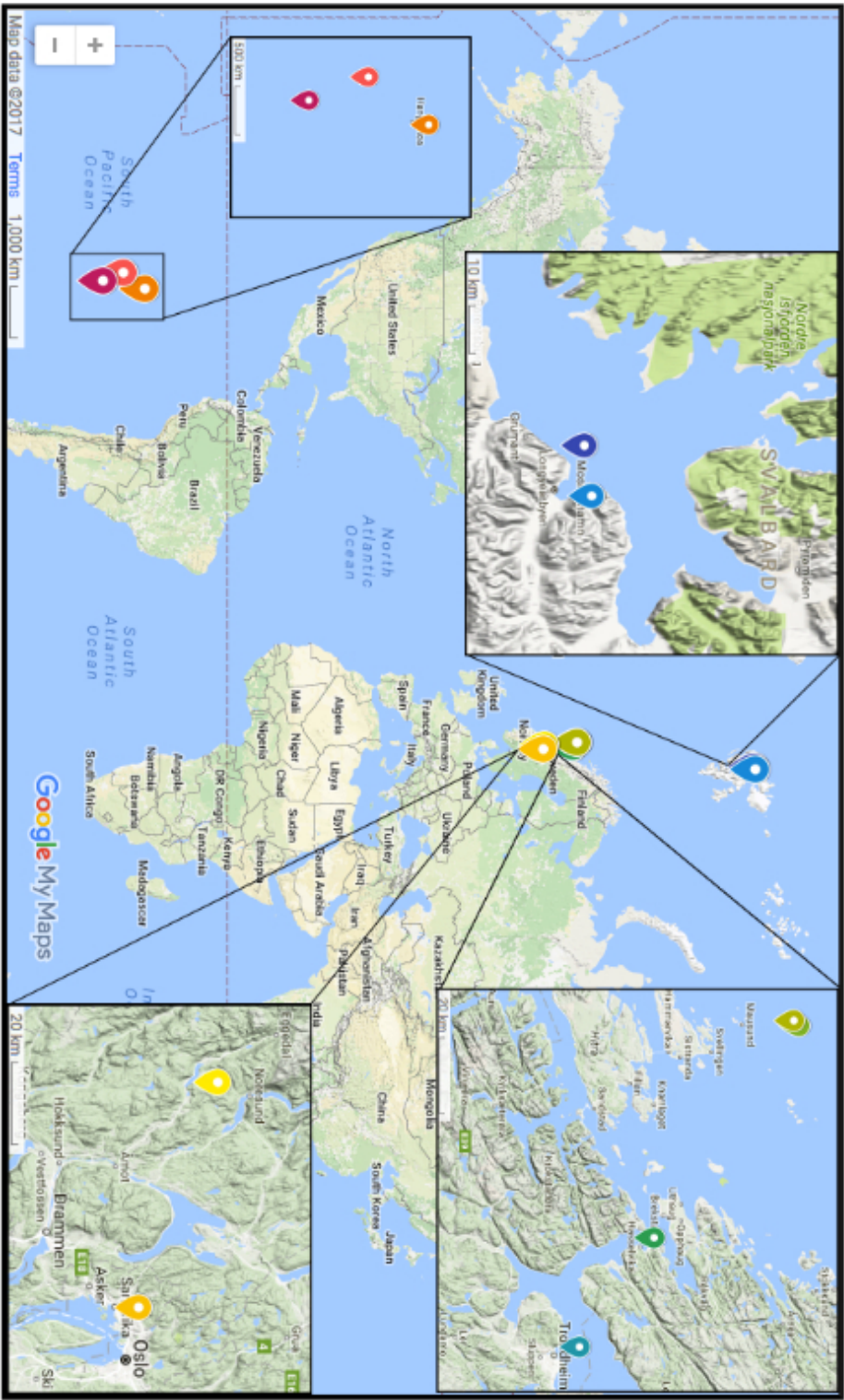


Figure 5: Map of sampling sites for this thesis. Map data from Google Maps.

## Field measurements of Secchi depth and Forel-Ule number, and water sampling

### Secchi Depth and Forel-Ule Measurements

The Secchi depth was used to obtain information of apparent optical properties in the water according to Wernand (2011). A white Secchi disk (diameter 30 cm) attached to a 50 m long braided nylon rope, diameter 0.5 cm, marked at every metre from the Secchi disk surface, was lowered into the water. Ideally this was done with the sun on the measurer's back, but more often, the current dictated the placement on the dock or vessel to avoid the Secchi disk disappearing from view under the dock or vessel. The depth at which the disk could no longer be seen was recorded, as well as the point where the disk could be seen again when hoisting it up. The depths were approximated to one decimal. The mean ( $n=2$ ) of these recordings was taken as the Secchi depth. The disk was then hoisted to half of the recorded Secchi depth, and ocean colour measurements were done using a plastic Forel-Ule scale from NIOZ (<http://forel-ule-scale.com/>), as well as the smartphone applications (apps) Citclops (<http://www.citclops.eu/>) and Eye On Water (<http://www.eyeonwater.org/>) on a smartphone. The Eye on Water app was released partway through the measurements for this thesis. The Citclops app was removed from app stores around this time as well. The measurements using the apps were done according to the instructions in the apps. Both apps ask for a picture of the ocean surface taken with the sun on the user's back, with the Secchi disk at half the Secchi depth visible in the measurement picture. This was not clear in the instructions for the Citclops app, and as a result most measurements using the app were done without the Secchi disk at half Secchi depth visible in the measurement picture. The user is then asked to select a part of the picture that is representative of the actual colour observed, or containing the Secchi disk. That part of the picture is then overlaid with colour bars corresponding to Forel-Ule colours that the user compares the picture to (see Appendix 1 for instructions provided by the apps). Separate pictures of the submerged disk were also taken at half the Secchi depth using a smartphone.

### Water samples

Water samples of 5 to 15 litres were taken from the surface using an acrylic glass tube sampler (1 m long, 10 L), effectively giving a sample from 0.2 to 1.2 m depth, or a bucket, giving a sample from 0 m to a maximum of 0.4 m depth. The water was kept cool and shaded until filtration and fixation, which happened within a maximum of 12 hours.

## Field measurements using instruments

### Rig construction

Several optical instruments were used to measure the optical qualities of the water, in conjunction with Forel-Ule measurements, such as an irradiance sensor, a spectroradiometer, and a fluorescence- and backscattering sensor. Rigs for the instruments were constructed using different materials to accommodate simultaneous logging using different devices. The rig constructed for continuous logging during the spring bloom period was connected to a buoy and kept at a constant depth of 3 m. Rigs for transects were made for measurements at Svalbard and Froan. These were lowered using a winch, measuring at specific depths. All irradiance and spectral irradiance measurements were conducted with the sensors pointing up, recording downwelling light. The lighting of the dock at TBS was turned off during in the spring bloom logging period to avoid the sensors being affected by artificial light.

### Irradiance, $E_{PAR}$

The irradiance  $E_{PAR}$  was measured using an Eco-Par sensor from Sea-Bird Scientific (Sea-Bird Scientific, Washington, USA). The Eco-Par is an autonomous instrument that measures irradiance ( $E_{PAR}$ ,  $\mu\text{mol quanta m}^{-2} \text{s}^{-1}$ ) in the visible part of the spectrum, i.e. photosynthetically active irradiance, PAR, 400-700 nm. The light collector was planar (a cosine-corrected  $\pi$  collector), measuring downwelling irradiance for 180 degrees above the sensor. The downwelling irradiance  $E_{PAR}$  was measured by pointing the light collector vertically upwards. The sensor was programmed to measure at different intervals according to use, once per second for measurements done when lowering rigs, or 10 times in quick succession every half hour for continuous logging during the spring bloom period.

### Spectral irradiance, $E(\lambda)$

Downwelling spectral irradiance was measured using a TriOS UV/VIS RAMSES (Radiation Measurement Sensor with Enhanced Spectral Resolution for the UV and visible spectrum) underwater spectrophotometer (TriOS, Oldenburg, Germany). It has a hyperspectral sensor with a 256 channel photodiode array sampling from 350 to 950 nm. Each measurement then gave values for the irradiance at each wavelength, calculated for 1 nm intervals. The instrument was connected to a laptop to instruct it to take samples using the interface programme Multi Sensor Data Acquisition, MSDA.

### Spectral transmission of Forel-Ule filters

To find the transmission of the plastic Forel-Ule filters, the downwelling spectral irradiance of light in air was measured through each Forel-Ule filter and a corresponding control measurement of the downwelling light at ground level. This was done in Longyearbyen, Svalbard.

### Concentration measurements of Chl $a$ , cDOM and TSM

Measurements of the main IOP components were done using the Eco-Triplet sensor from Sea-Bird Scientific (Sea-Bird Scientific, Washington, USA). The sensor measures inherent optical properties of the water by the use of internal light sources. The different variables, the concentration of Chlorophyll  $a$  ([Chl  $a$ ],  $\mu\text{g L}^{-1}$ ), coloured Dissolved Organic Matter (cDOM, ppb) and Total Suspended Matter (TSM, Beta,  $\text{m}^{-1} \text{sr}^{-1}$ ), were measured by emitting and measuring light at different wavelengths, as shown in Table 2. The emitters for each channel are placed at 90 degrees to the measuring sensors to avoid interference from the emitted light. These measurements were done to create a reference between the measured AOPs and IOPs, which are the components of interest to biologists and others. The variable used to measure the amount of TSM was Beta, the coefficient of the volume scattering function (Watson and Zielinski 2013). Its units are per metre per steradian ( $\text{m}^{-1} \text{sr}^{-1}$ ), in which the steradian can be considered a unit of volume (Watson and Zielinski 2013). For ease of comparison, Beta was multiplied by 1000 before use.

During the spring bloom logging period the Eco-Triplet device was set up to log ten times in quick succession each half hour, and these ten measurements were treated as parallels and means of the parallel measurements were calculated before use. Breaks in the data are due to recalibration and maintenance of the device.

Table 2: Wavelengths used for measuring the variables from the ECO-TRIPLET

Variable measured	Excitation $\lambda$ (nm)	Emission $\lambda$ (nm)
[Chl $a$ ]	470	695 (fluorescence)
[cDOM]	370	460 (fluorescence)
Beta	700	700 (light scattering)

### Temperature, salinity and depth

The temperature, salinity and depth were measured using a CTD (SAIV SD 204 STD/CTD and CastAway CTD from SonTek YSI), which stands for Conductivity, Temperature, Depth.

The conductivity of the water is usually converted into salinity (psu, practical salinity unit), and the depth (m) is calculated from the pressure measured by the CTD. The CTD was either used to take a transect on its own, or connected to a rig with the other instruments for accurate depth measurements.

## Lab work

### Filtration and fixation

Within 12 hours of the water sample being collected, most often within 2-4 hours, 0.5 – 2.5 L of the sample was filtrated through Whatman GF/F glass-fibre filters with a diameter of 25 mm using a vacuum. The filtering unit differed between sites, but there were generally three filtering units connected to the same water vacuum pump. The water was pumped into the water vacuum pump, which had an overflow tube. Aboard R/V Gunnerus, the pump was connected to a large glass flask to which one filtering unit (Gelman Sciences) was connected. The sample was introduced to a container above the filter, which was lying on top of a plastic grid in a plastic holder. The plastic holder narrowed to a tube that was stuck through a silicone stopper. The stopper connected snugly to an opening on the flask or three-filtering unit. The water was gently mixed before measuring, by upending the closed container with the sample 7 times. If the sample was stored in a bucket, a measuring cup or similar was used to mix the water before the sample was taken out. Water was added until the filter showed visible colouration, and the volume noted. As soon as the filtration was completed, the filter was removed from the filtrating apparatus, folded once, stored in a vial (2 mL) or folded into aluminium foil, then immediately frozen in a freezer at -20 °C.

200 mL of each sample was fixated using 2 mL Lugol's solution at the beginning, later using neutral iodine solution, also known as non-acidic Lugol's solution. The fixated samples were kept in brown glass bottles in a cupboard at room temperature and were used for cell counting.

The pigments from the frozen filters were extracted using 1.6 mL methanol in glass vials (2 mL), before being shaken down using a vortex mixer to make sure the filters were covered in methanol. Standard procedure in this case would be to replace the air in the vials with pure nitrogen gas to avoid oxidation of the pigments. This was not performed in this project, because the amount of air was considered too small for oxidation to occur. The filters were extracted overnight at -20 °C. At the end of the extraction period the extracts were refiltered

through a 13 mm syringe filter (0.2 µm pore size, PTFE) to avoid debris and filter material prior to pigment analysis (Rodriguez et al. 2006).

### Phytoplankton pigments

The High Precision Liquid Chromatography instrument (Hewlett Packard Agilent 1100) equipped with a Water Symmetry C8 (4,6\*150 mm, 3,5 µm pore size) column which separated the pigments in time based on polarity was used for pigment analysis, using the method of Rodriguez et al. (2006). A cleaning procedure was always used before starting sampling as detailed in Rodriguez et al. (2006). Several vials containing samples were placed at once in a cooled tray (4 °C), and the HPLC was programmed to sample each using a connected computer. The absorbance of the pigments was measured using a diode array.

The concentrations of pigments, here denoted  $p$ , found when doing HPLC analysis were calculated using the integrated value for the area under the sensor curve at 440 nm, denoted  $A$ . The filtered volume is denoted  $V_f$  and the extracted volume is denoted  $V_{ex}$ , and both are given in mL. The reference value for pigment  $p$  is denoted  $Rf_p$ , and found by calibration or calculation. The resulting concentration has the units  $\mu\text{g L}^{-1}$ .

$$[p] = \frac{A \times Rf_p \times V_{ex} \times 1000}{77 \times V_f} \quad \text{Equation 1}$$

### *In vitro* [Chl $a$ ]

The fraction of sample not used for HPLC analysis was diluted by half. A Turner Designs Trilogy fluorometer with the fluorescence module Chlorophyll  $a$  (Non-Acid) (485 nm excitation filter, 685/10 nm emission filter) was used as an additional measure of the concentration of Chlorophyll  $a$  in the sample. The fluorescence module used was for non-acidic extracts of Chlorophyll  $a$ .

### Sedimentation and counting (Utermöhl method)

A column for Utermöhl method (Utermöhl 1958) was connected to a bottom plate using wax. The sample flasks containing Lugol-fixed samples were turned gently for 1 minute before enough sample to fill the column was poured along the side of the column until the sample was bulging over the top. A top plate was slid across the top of the column. The column was standing on a plane surface. It was left for 12-24 hours before a glass plate was slid across the

bottom plate using water as a film between the column and the plate. The sample, ready for counting, was kept as level as possible upon transfer to the microscope.

A microscope (Leica DM IRB) with a camera (SONY DFW-X700, Axiocam 105 color) connected to a computer was used. This made it possible to take pictures of the algae seen in the microscope. Counting was done using the built-in measuring scale in the ocular of the microscope as guidance, counting every cell falling within the measuring scale in a vertical or horizontal stripe. According to the cell density, half the bottom plate was counted, counting every other stripe, or one stripe vertically down the middle, sometimes followed by a horizontal stripe across the middle. Cells lying halfway into the stripe were counted on one side of the stripe and not on the other side. At 400x magnification, fields of view were counted, meaning every cell within the circular view in the microscope was counted. The cells were put into categories of species, genus, family or order according to what level of identification was possible using the light microscope. Larger species were counted at 200x magnification, and smaller species at 400x magnification. Lower cell size limit at 400x magnification was around 5  $\mu\text{m}$  (Edler and Elbrächter 2010).

### Data processing

In sensor data with replicate measurements, a mean of the replicates was calculated. This includes the optical data for Chl *a*, cDOM and TSM concentrations, PAR irradiance and spectral irradiance. This is also the case for the three parallels of pigment samples in HPLC, though the mean was calculated after calculating concentrations.

### Calculating the attenuation coefficient

The light attenuation coefficient was calculated from the Secchi depth, irradiance in the PAR spectrum at different depths, and spectral irradiance at different depths. The formulas used are as follows.

The empirical coefficient 1.7 (Sakshaug et al. 2009b) was used to calculate the  $K_d$  for the water from the Secchi depth,  $S_d$ , using the following formula.

$$K_d = \frac{1.7}{S_d} \quad \text{Equation 2}$$

The calculation of the  $K_d$  using irradiance in the visible spectrum,  $E_{PAR}$ , was done using the following formula, where  $Z_1$  is the shallower depth and  $Z_2$  is the deeper depth.

$$K_d = \ln \left( \frac{E_{Z_2}}{E_{Z_1}} \right) / (Z_2 - Z_1) \quad \text{Equation 3}$$

The calculation of the  $K_d(\lambda)$  using the spectral irradiance data was done in a similar way for each wavelength, according to the following formula.

$$K_d = \ln \left( \frac{E_{\lambda(Z_2)}}{E_{\lambda(Z_1)}} \right) / (Z_2 - Z_1) \quad \text{Equation 4}$$

To be able to compare the  $K_d$  values, an  $E_{PAR}$  value was created from the values for each wavelength of the  $E(\lambda)$  from 400 nm to 700 nm. This was done using the equation below.

$$K_d = \ln \left( \frac{\sum_{PAR} E_{\lambda(Z_2)}}{\sum_{PAR} E_{\lambda(Z_1)}} \right) / (Z_2 - Z_1) \quad \text{Equation 5}$$

### Calculating transmission of light through Forel-Ule filters

The normalised transmission of light through the plastic Forel-Ule filters were calculated using the method shown in Wernand (2011).

This method is repeated below for clarity. The spectral transmission through each Forel-Ule filter,  $T_{FU}$ , was calculated by dividing the irradiance measured through the Forel-Ule filter, denoted as  $E(\lambda)$ , by the spectral irradiance from the sun measured directly after the filter measurement, denoted  $E_0(\lambda)$ .

$$T_{FU}(\lambda) = \left( \frac{E(\lambda)}{E_0(\lambda)} \right) \quad \text{Equation 6}$$

For easy comparison, the spectral transmission was then normalised to the maximum value of  $T_{FU}$  found between 380 and 780 nm, denoted  $T_{FU, MAX}$  (Equation 7). This wavelength interval



is used for ease of comparison with values in Wernand (2011). The calculation of  $T_{\text{FUN}}$  is shown in Equation 8.

$$T_{\text{FU, MAX}} = \text{MAX}(T_{\text{FU}}, \lambda \in [380, 780]) \quad \text{Equation 7}$$

$$T_{\text{FUN}}(\lambda) = \frac{T_{\text{FU}}(\lambda)}{T_{\text{FU, MAX}}} \quad \text{Equation 8}$$

## Results

### Spring bloom time series of AOPs and IOPs

The spring bloom time series was conducted at TBS from the 8<sup>th</sup> of March until the 8<sup>th</sup> of April. The mean  $E_{PAR}$  between 11:00 and 13:00 for each day at 3 m depth varied greatly, with no clear increasing trend, as shown in Figure 5.

Figure 5 shows the Secchi depth and Forel-Ule number as measured from the dock at TBS from the 8<sup>th</sup> of March till the 8<sup>th</sup> of April 2016.

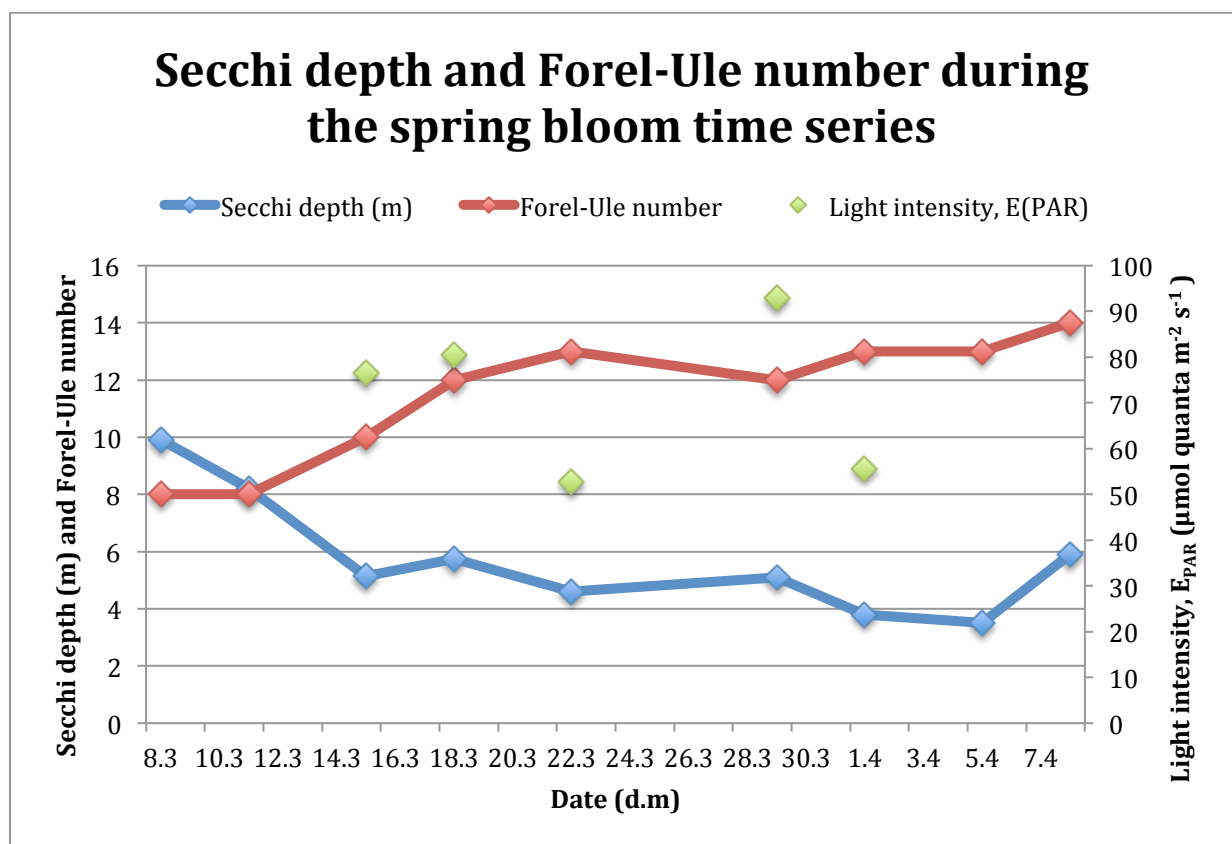
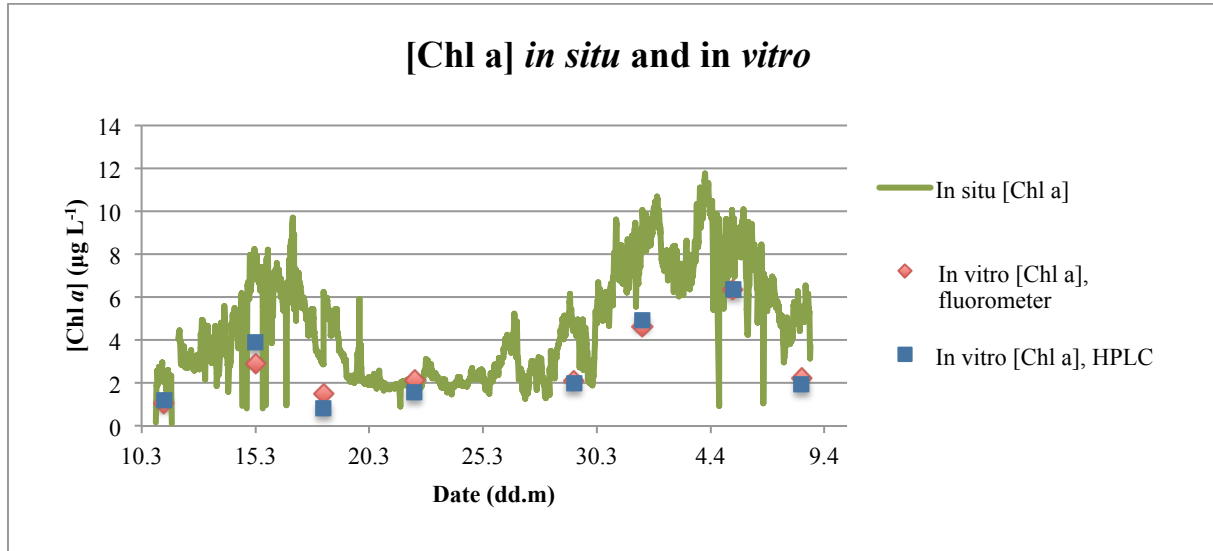


Figure 5: The Secchi depth and Forel-Ule number as measured from the dock of TBS from 8<sup>th</sup> of March to 8<sup>th</sup> of April 2016. The mean  $E_{PAR}$  from 11:00 to 13:00 is shown on the secondary axis.

The graph in Figure 6 shows the [Chl *a*] measured *in situ* and *in vitro*. The *in situ* measurements are from fluorescence data. The *in vitro* measurements were done after pigment extraction, and were carried out using both a Turner Designs fluorometer, and HPLC.

There appears to be two peaks of [Chl *a*] in this data. The maxima of these according to *in situ* data were around the 16<sup>th</sup> of March and the 3<sup>rd</sup> of April. The *in situ* maxima measured were 9.72  $\mu\text{g L}^{-1}$  Chl *a* for the first peak and 11.8  $\mu\text{g L}^{-1}$  Chl *a* for the second peak.



**Figure 6: Chlorophyll *a*, [Chl *a*] measured *in situ* using an ECO-TRIPLET instrument, and measured *in vitro* by filtering seawater and extracting the pigments from the resulting filter using methanol, followed by measurement using a Turner Designs fluorometer.**

The amounts of TSM and cDOM were also measured during the spring bloom series, see Figure 7. The covariation of cDOM and TSM was checked by dividing [cDOM] by the measure of the amount of TSM, which, when two outliers were removed, had a mean of 2.21 and a standard deviation of 0.85.

During the spring bloom time series, there was an increase in the amounts of cDOM and TSM between the blooms, from the 21<sup>st</sup> to the 27<sup>th</sup> of March, and during the second bloom, from the 3<sup>rd</sup> of April until the end of the measurements done, on the 8<sup>th</sup> of April.

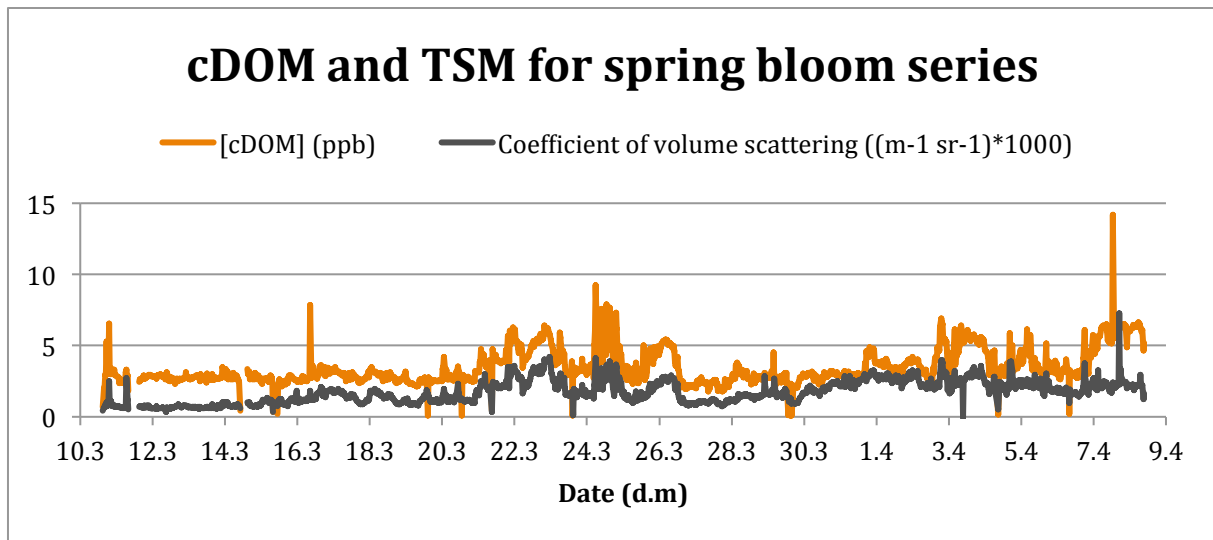


**Figure 7: The [cDOM] and the coefficient of volume scattering during the spring bloom series, measured *in situ* using the ECO-TRIPLET. The coefficient of the volume scattering function is used here as a measure of the amount of TSM in the water.**

The *in situ* [cDOM], [Chl *a*] and TSM amounts from the spring bloom time series were used as predictor variables for the Forel-Ule data. This was done by first picking the relevant points for comparison, ending up with relatively few data points ( $n=8$ ). A linear regression model selection was carried out using the "shotgun" method, trying all combinations of the predictor variables. This method was possible to do due to the low number of predictor variables. In this modelling, the Beta variable was not multiplied by 1000 first. The predictor variables were mean-centered for ease of comparison and interpretation. This was done by dividing all data points in a series by the mean of the same series. A model using only Chl *a* as a predictor variable showed that the concentration of Chl *a* did not significantly explain the change in Forel-Ule number ( $p=0.8308$ ). The final model was a model including both cDOM and TSM, which considered interactions between these predictor variables. Models using the untransformed data were made for each variable, and plots of the models using cDOM and TSM are shown in Figure 8.

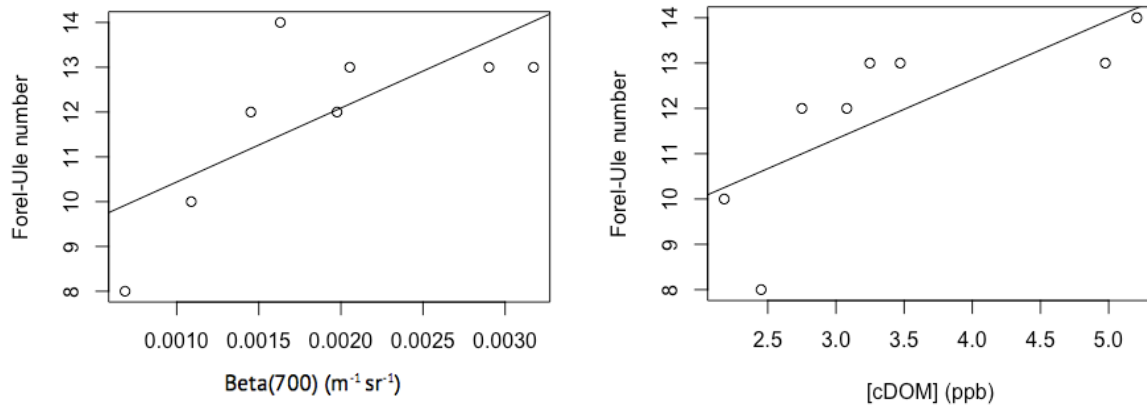


**Figure 8: The data points and linear models for models using TSM (left) and cDOM (right) as predictor variables for Forel-Ule number during the spring bloom series.**

Table 3 shows the parameters of the final model, using cDOM and TSM and their interaction to explain the change in Forel-Ule number. The influences of cDOM, TSM and their interaction are all significant to 0.05. The intercept is more unsure, with a standard error more than ten times that of the estimated value. The impact on Forel-Ule numbers by the predictor variables was estimated by multiplying the range of values in the mean adjusted series with the corresponding estimated coefficient. The range of the mean-adjusted TSM data were found to be 1.33, while the range of the cDOM data was smaller, at 0.885. Using this method, TSM was found to have a greater possible impact on the Forel-Ule number than cDOM. More details of the model are shown in Appendix 2.

Table 3: The size of the intercept and the coefficients which explain the Forel-Ule number in the final model. These coefficients are cDOM, TSM, and a strong interaction between these two, likely explained by a common underlying source. The adjusted R-squared value, which describes the proportion of variation in the Forel-Ule number explained by the model, is 0.8185. Pr-values, the probabilities of the relationships to be results of random chance, fall below 0.05, the threshold of significance, for all three coefficients. The intercept is much less certain and much be treated as an approximate figure.

<b>Coefficients</b>	<b>Estimate</b>	<b>Std. Error</b>	<b>t value</b>	<b>Pr(&gt; t )</b>
<b>(Intercept)</b>	0.2023	2.5344	0.080	0.9402
<b>Mean.cdom</b>	10.0373	2.6702	3.759	0.0198
<b>Mean.beta</b>	9.6794	2.7810	3.481	0.0253
<b>Mean.cdom:mean.beta</b>	-7.4634	2.5069	-2.977	0.0409

Phytoplankton cell counts were performed for the sample dates of the spring bloom series. Two blooms, corresponding to the ones shown in Figure 6, were observed from the cell count data. The maximum cell concentration in each of the blooms were found on the 15<sup>th</sup> of March and the 1<sup>st</sup> of April, with 3280 and 6826 cells mL<sup>-1</sup> respectively. The two blooms had different phytoplankton species compositions, with the first one being dominated by the dinoflagellate *Heterocapsa rotundata*, and the second one by the diatom *Skeletonema costatum*, see Table 4. The concentrations of the main phytoplankton groups during the spring bloom series are shown in Figure 9.

**Table 4: The concentrations (cells mL<sup>-1</sup>) of the taxa with >100 cells mL<sup>-1</sup> for one sample or more during the spring bloom series. Darker green colour indicates a higher concentration.**

Taxon	8.3	11.3	15.3	18.3	22.3	29.3	1.4	5.4	8.4
Cryptophyte	116	232	257	89	47	29	228	97	66
Flagellate	295	647	1062	394	399	455	1348	1203	772
<i>Heterocapsa rotundata</i>	95	188	1734	38	114	14	166	83	50
<i>Skeletonema costatum</i>	32	11	76	147	179	466	2482	3049	198
<i>Chaetoceros curvisetus</i>	13	12	32	17	5	0	181	0	0
<i>Chaetoeros socialis</i>	0	0	0	0	0	538	773	882	32
<i>Chaetoceros</i> sp.	2	1	4	24	104	322	910	210	45
<i>Chaetoceros</i> sp. resting spores	0	0	0	0	0	79	181	7	0
Small centric diatoms, unidentified	0	0	0	0	3	0	426	25	19

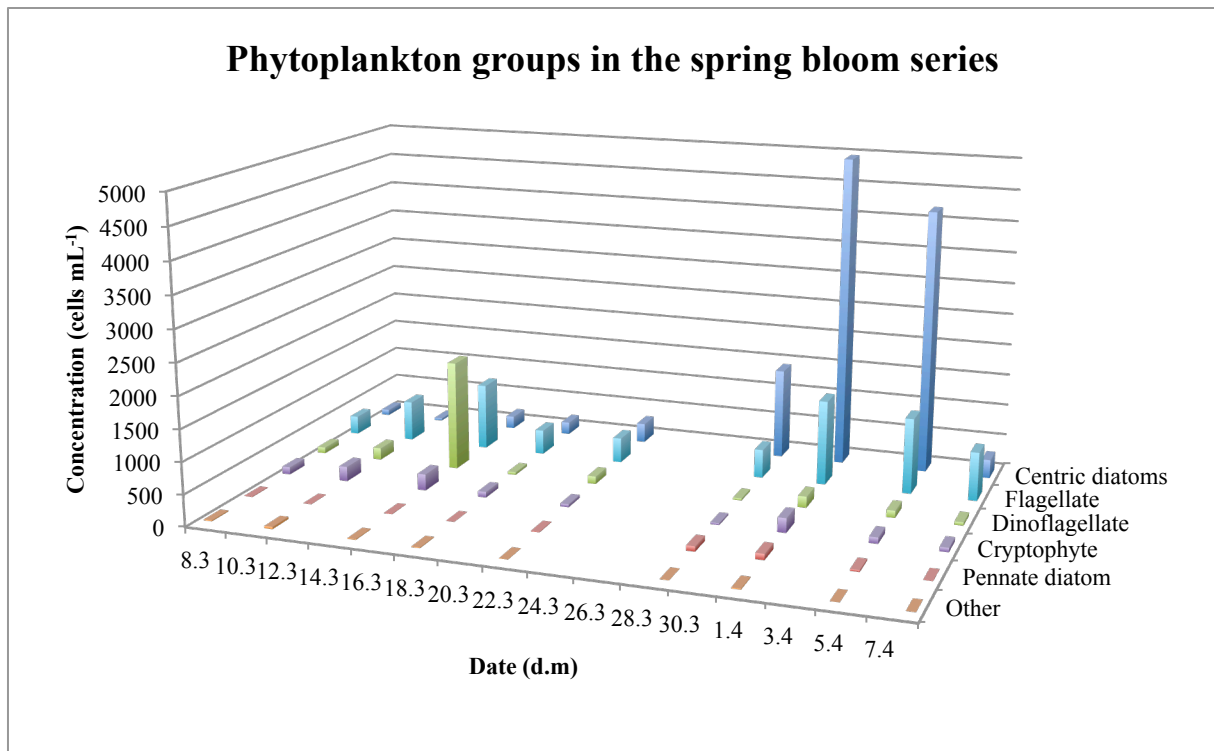


**Figure 9:** The concentrations (cells mL<sup>-1</sup>) of algal groups in seawater samples taken from the 8<sup>th</sup> March to the 8<sup>th</sup> April from the dock at TBS, counted using the Utermöhl method.

Figure 10 shows the concentrations of the light harvesting and photoprotective pigments found in the spring bloom series. The light harvesting pigments found were Chlorophylls *a*, *b*, *c*<sub>1</sub>, *c*<sub>2</sub> and *c*<sub>3</sub>, Fucoxanthin and Peridinin. The only photoprotective pigment found in large enough amounts was Diadinoxanthin. Peridinin, a biomarker for dinoflagellates, was found during the first bloom, but not during the second bloom. More Chl *b*, a bioindicator of chloro- prasino- and euglenophytes, was found during the first bloom than during the second bloom. Fucoxanthin, Chl *c*<sub>1</sub> and Chl *c*<sub>2</sub> were found at high concentrations during the second bloom, indicating the presence of Chromophyta.

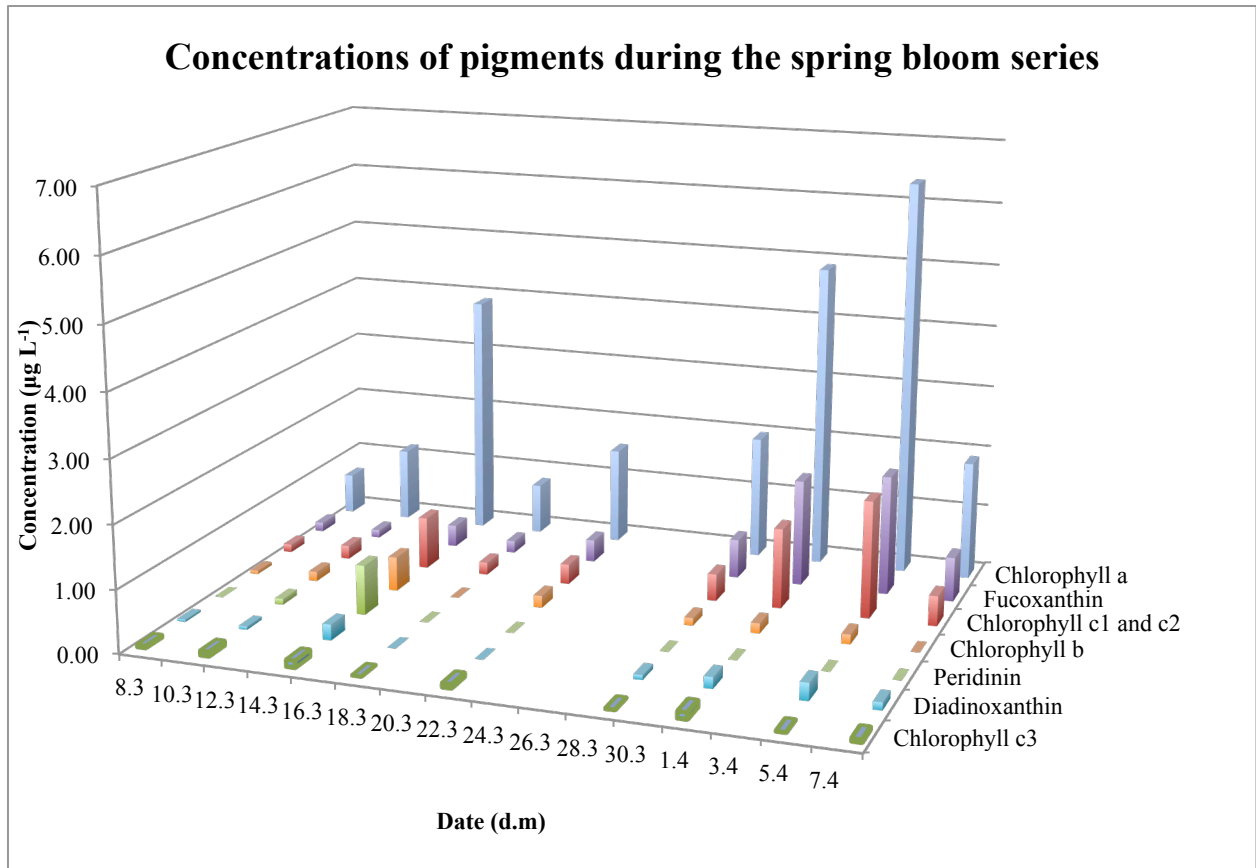


Figure 10: Concentration of pigments in seawater samples taken from the 8<sup>th</sup> March to the 8<sup>th</sup> April from the dock at TBS, from HPLC analysis.

### Evaluation of the Forel-Ule scale

Figure 11 shows the connection between Secchi depth and Forel-Ule number. It includes all measurements done for this thesis, in waters as disparate as the South Pacific Ocean and a freshwater lake in Norway, and the fitted trend line is a power trend line, which is a trend line of the type  $y=cx^b$ , where  $c$  and  $b$  are constants.



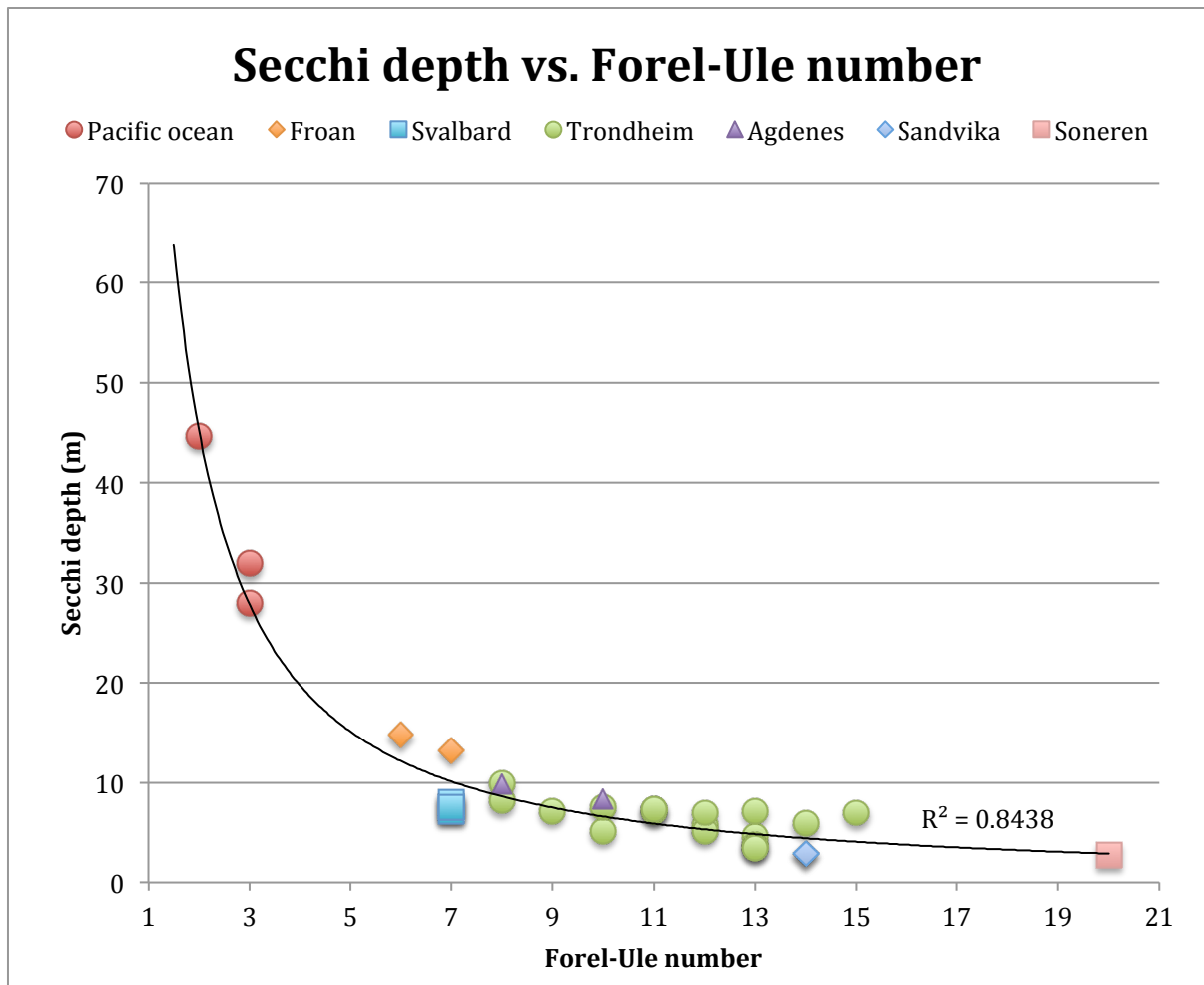


Figure 11: All Secchi depth measurements from this master project shown as a function of Forel-Ule number, with a power trend line of the form  $y=cx^b$ , with  $R^2=0.8438$ .

In Figure 12, the Secchi depth measured during the spring bloom series is shown together with the Forel-Ule measurements, but these have been inverted. This has been done by subtracting the measured Forel-Ule number from 21, the largest Forel-Ule number. This has been done to be able to compare more directly the Secchi depth and the Forel-Ule number. Figure 13 shows the difference between these, the Secchi depth and the inverted Forel-Ule number, to see the part of the Forel-Ule number which is not determined by the Secchi depth, (hereby called the Forel-Ule No Secchi, or FUNS, factor). The calculation of the FUNS factor is shown in Equation 9, where  $FU_{MAX}$  denotes the maximum Forel-Ule number, 21,  $FU$  denotes the Forel-Ule number measured, and  $Sd$  denotes the Secchi depth measured. The FUNS factor is shown together with the *in vitro* measurements of [Chl *a*] found using HPLC in Figure 13.

$$FUNS = FU_{MAX} - FU - Sd$$

Equation 9

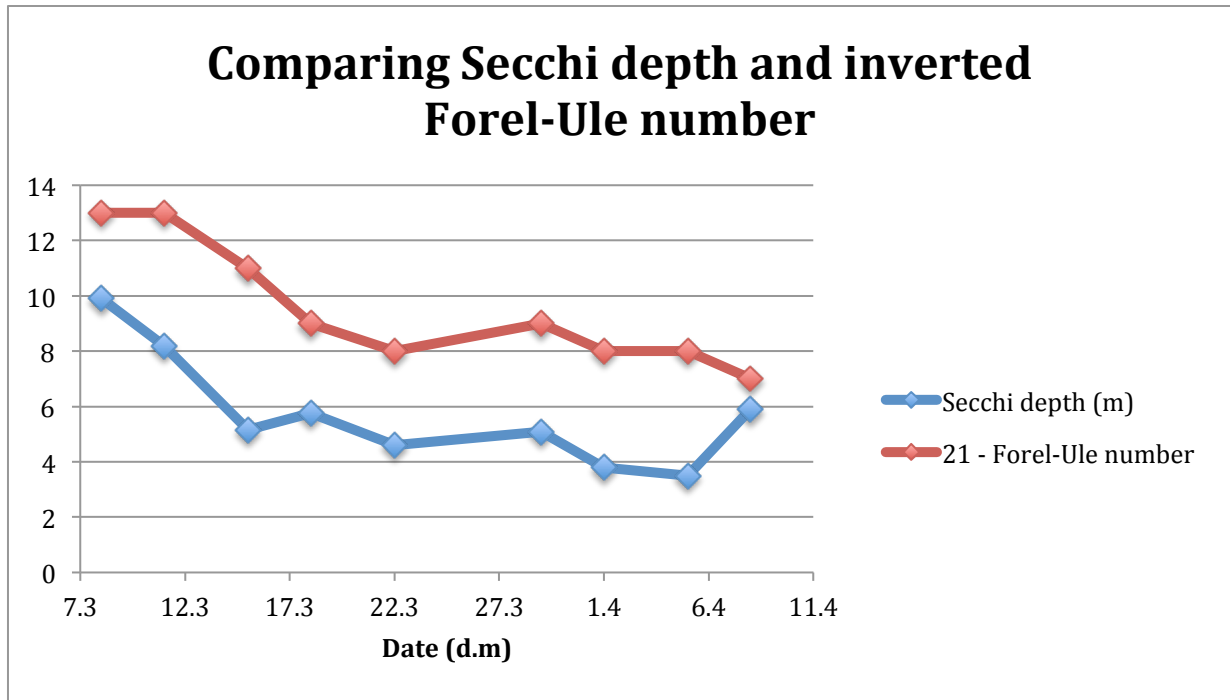


Figure 12: Secchi depth and Forel-Ule numbers for the spring series measured at TBS, where Forel-Ule numbers are shown inverted, as 21 minus the Forel-Ule number.

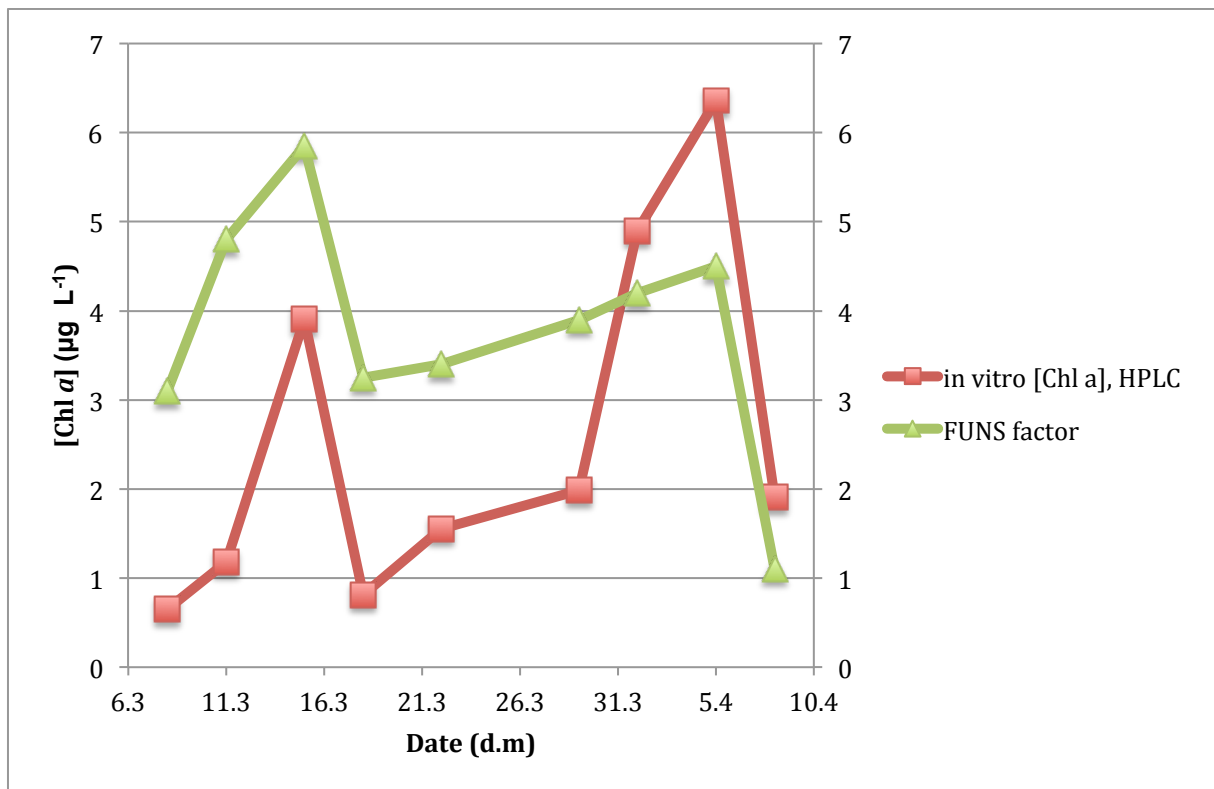


Figure 13: The factor of 21 minus Forel-Ule number minus Secchi depth, the difference between Secchi depth and the inverted Forel-Ule numbers, the FUNS factor, shown on a secondary axis, with the *in vitro* measurement of [Chl a] using HPLC shown on the primary axis. The FUNS factor is created to be able to examine the part of the Forel-Ule number not determined by Secchi depth.

Figure 14 shows [Chl *a*] found using HPLC (top) and cell concentrations (bottom) shown as a function of Forel-Ule number. These figures show the amount of phytoplankton, using two proxies for biomass, found in water categorised into different Forel-Ule numbers.

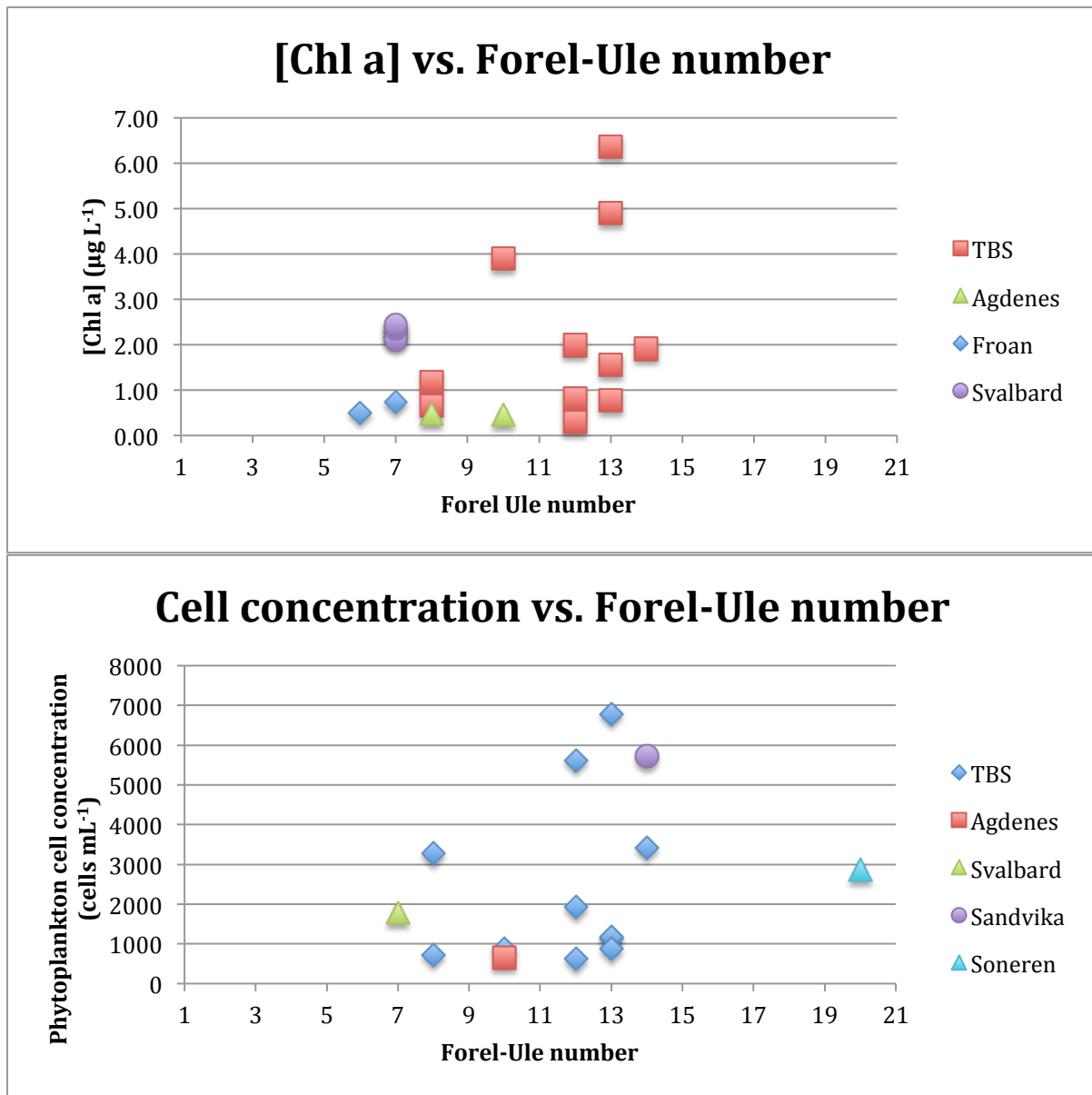


Figure 14: [Chl *a*] (top) and total cell concentration (bottom) shown as a function of Forel-Ule number. Different colour points indicate different locations.

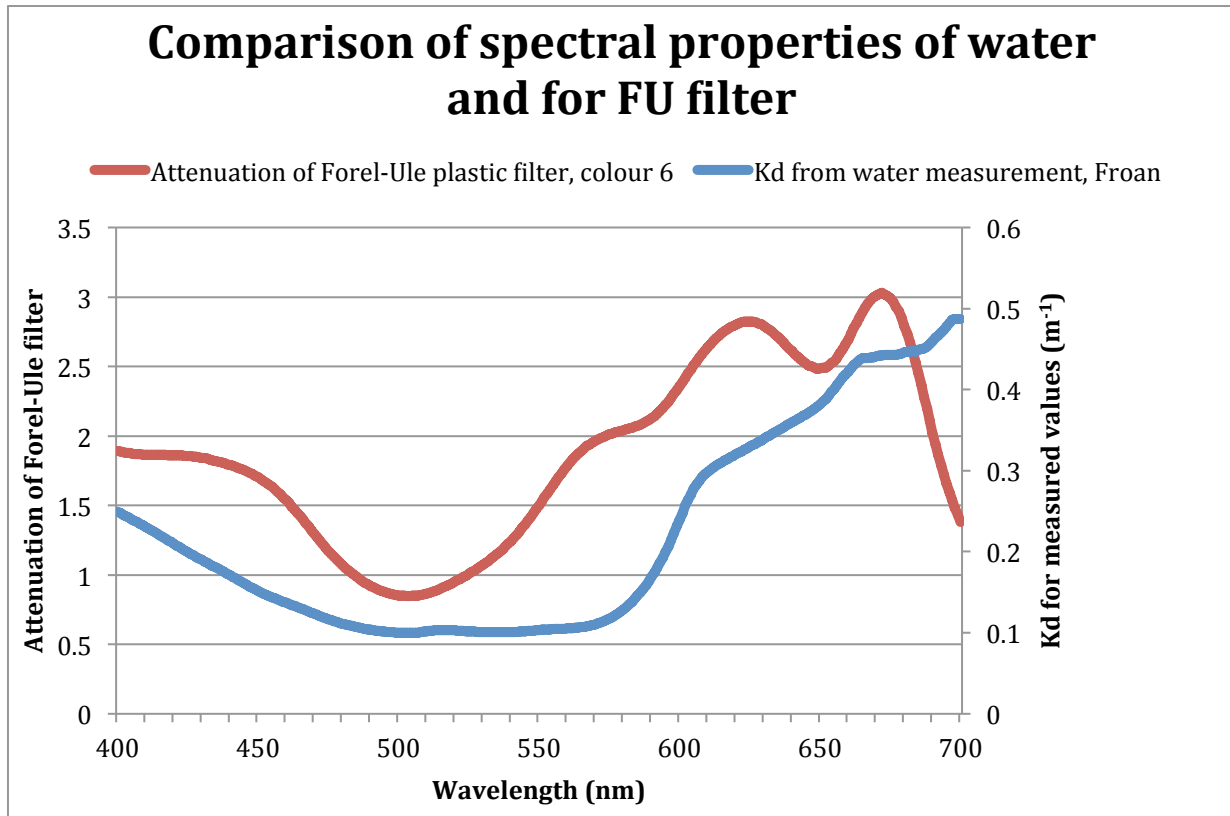
$K_d$  values for the visible spectrum can be calculated using data from different methods, see Equations 2, 3, 4 and 5. Table 5 shows that the calculated values of the attenuation coefficient  $K_d$  from this project are generally in agreement between methods and instruments, except the

calculations using the Secchi depth at Svalbard. Those calculations are generally lower than the values found using modern optical methods.

**Table 5:  $K_d$  calculated using different gathered data.**

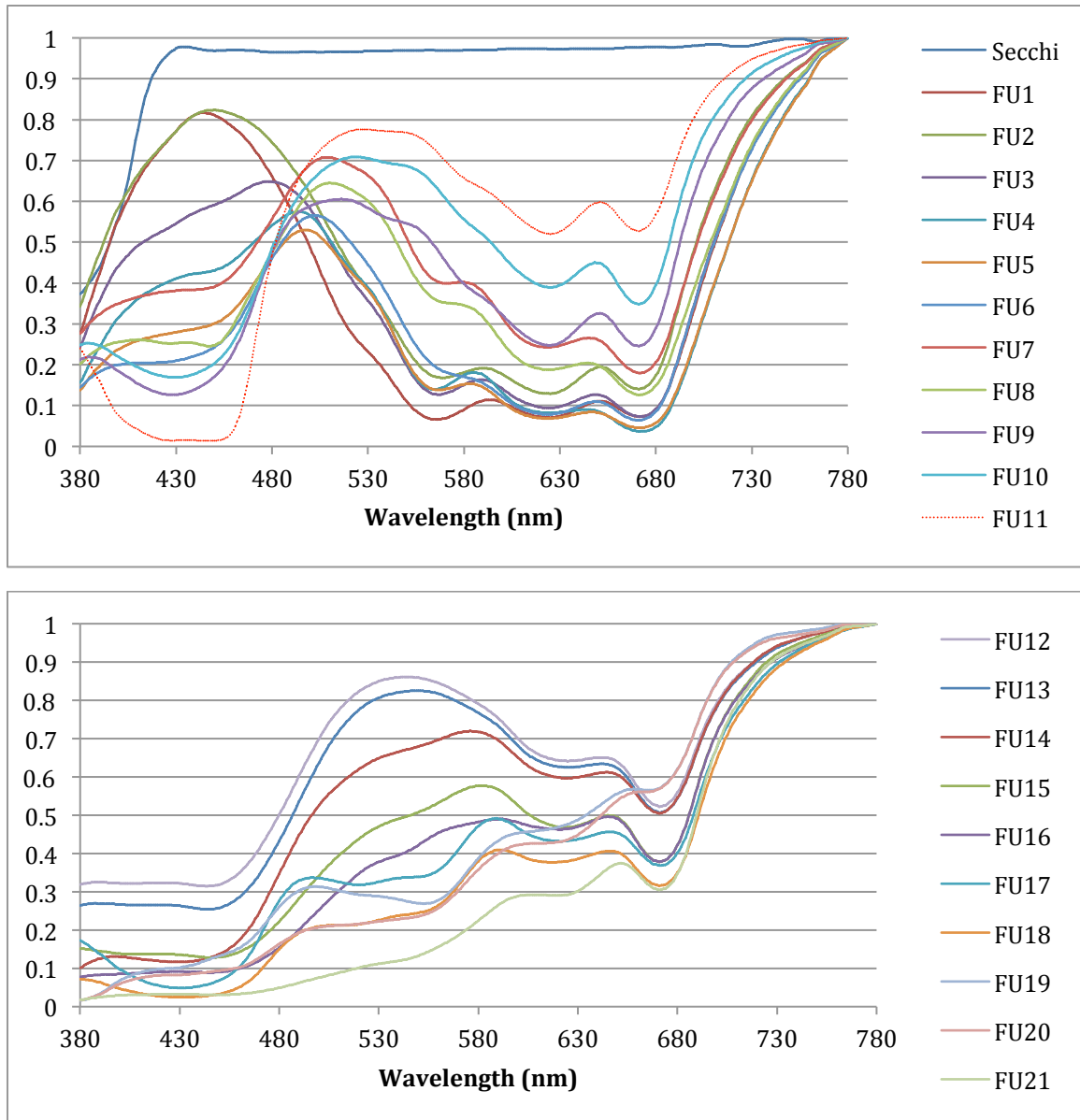
<b><math>K_d</math> using</b>	<b>Svalbard</b>	<b>Svalbard</b>	<b>Svalbard</b>	<b>Froan st. 1</b>	<b>Froan st. 2</b>
	<b>10.5</b>	<b>11.5</b>	<b>13.5</b>		
<b>Secchi depth</b>	0.23	0.21	0.23	0.13	0.12
<b><math>E_{PAR}</math></b>	0.30	0.26	0.31		
<b><math>E(\lambda)</math> integrated from 400 to 700 nm</b>	0.31	0.26	0.31	0.14	0.12
<b><math>E(\lambda)</math> integrated from 400 to 700 nm, corrected for surface <math>E_{PAR}</math></b>				0.13	0.13

Figure 15 shows a comparison of the spectral properties of water measured to have Forel-Ule colour 6 and the physical Forel-Ule filter number 6. It shows the spectral attenuation of the Forel-Ule filter, and the  $K_d$  of the water from the surface to Secchi depth.



**Figure 15:** The spectral attenuation coefficient of water measured ( $\text{m}^{-1}$ ) to have Forel-Ule colour number 6, and the spectral attenuation of the corresponding plastic filter of the physical Forel-Ule measuring device. Water measurements done at Froan.

Figure 16 shows the normalised transmission spectra from the physical Forel-Ule filters used for measurement of the Forel-Ule number during this thesis, and the normalised reflectance of the Secchi disk (white polyethylene). These values were calculated according to the method described in Wernand (2011), see Equations 6, 7 and 8. A measurement error leads to the curve for FU11 being untrustworthy. There are peaks in the transmission for most filters at about 645 nm and 580 nm, and troughs at about 618 nm and 666 nm.



**Figure 16: The transmission spectra of the plastic Forel-Ule filters, calculated and normalized using the method described in Wernand (2011). The reflectance of the Secchi disk is also included.**

Pictures taken using a smartphone camera of the Secchi disk at half the Secchi depth are shown in Figure 17. For both measurements, the water was categorized as Forel-Ule colour number 8. These pictures are from the 11<sup>th</sup> of March at the dock at TBS, and from the 21<sup>st</sup> of April at Agdenes taken from R/V Gunnerus. Allowances for currents had to be made when doing both these measurements, so the sun ended up shining in the measurer's face for both these measurements.



**Figure 17: Two pictures of the Secchi disk at half the Secchi depth on different days. The ocean colour was categorized to the same Forel-Ule number, number 8. The left one is from the 11<sup>th</sup> of March from the dock at TBS, and the right one is from the 21<sup>st</sup> of April from R/V Gunnerus at Agdenes.**

### **Evaluation of the use of the Forel-Ule scale for citizen science**

User tests, where eight different people measured the Secchi depth and Forel-Ule number within an hour of each other, as described in materials and methods, show a broad spread of results, see Figure 18. The mean Secchi depth measured was 7.2 m, with a relatively low standard deviation of  $\pm 0.2$  m. The Forel-Ule measurements, with a mean of 11.5, had a much higher standard deviation of  $\pm 1.9$ . The spread of measurements is shown in Figure 18. None of the participants were colour blind, but a front was observed passing the dock during measurements.

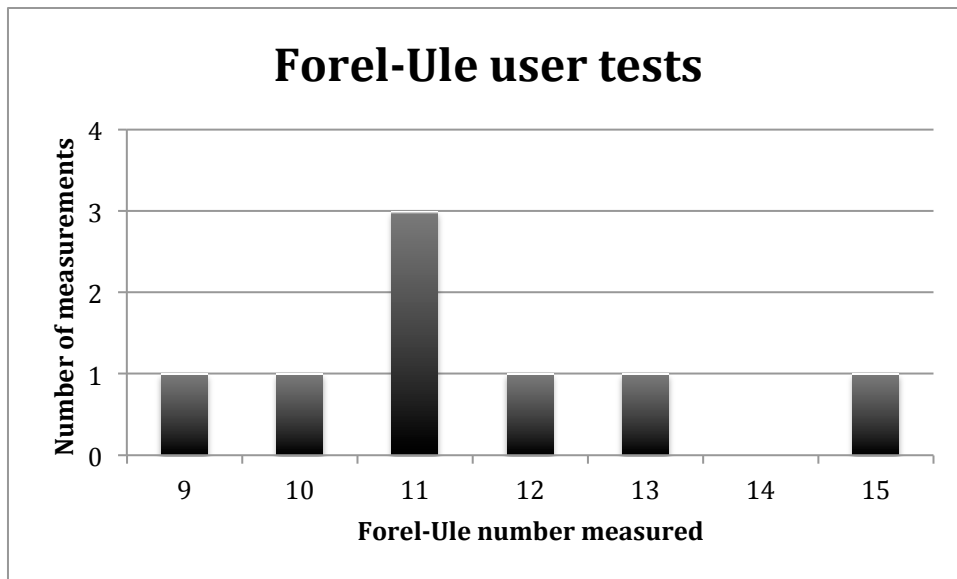


**Figure 18:** The results from user tests, where 8 different people measured the Forel-Ule number using the physical scale within a time window of about 1 hour.

Most measurements using apps were taken using the Citclops app and not including the Secchi disk at half Secchi depth in the measurement picture (see Table 6). The mean (n=13) absolute difference between the measurements using the physical Forel-Ule scale and using the Citclops app without a Secchi disk was 4.2, with a standard deviation of 2.0.

**Table 6:** Forel-Ule measurements using the smartphone apps Citclops and Eye on Water both with and without a Secchi disk, shown together with measurements done using the physical Forel-Ule scale. The mean absolute difference between the measurements using the physical Forel-Ule scale and the measurements using the Citclops app without a Secchi disk is 4.2, with a standard deviation of 2.0.

Date	Place	Physical Forel-Ule scale	Citclops app without Secchi disk	Citclops app with Secchi disk	Eye on Water app without Secchi disk	Eye on Water app with Secchi disk
8.3	TBS	8	4			
11.3	TBS	8	6			
15.3	TBS	10	7			
18.3	TBS	12	7			
22.3	TBS	13	8			
1.4	TBS	13	8			
5.4	TBS	13	9			
8.4	TBS	14	9			
18.4	Agdenes	10	8			
21.4	Agdenes	8	4			
26.4	TBS	12	5	12		
7.6	Froan	7			6	6
7.6	Froan	6			5	5
24.6	Sandvika	14	6		7	15
28.7	Soneren	20	21	18	20	17



## Discussion

### Spring bloom time series of AOP and IOP

Both *in situ* Chl *a* fluorescence, and HPLC and fluorescence measurements of *in vitro* [Chl *a*] indicate two peaks of phytoplankton biomass during the time series (08.03.16-08.04.16). This is also in agreement with the results from cell counts and phytoplankton pigment concentrations. This pattern indicates that two phytoplankton blooms happened during this time series. This two-peak pattern is not, however, observed for the Forel-Ule number and the Secchi depth. During the time series, the Forel-Ule number increases, and the Secchi depth decreases, with no clear two-peak pattern.

The *in vitro* [Chl *a*] were generally lower than *in situ* measurements. The two *in vitro* measurements of [Chl *a*] using the fluorometer and HPLC are very similar. The most likely reason for this is a calibration error in the ECO-TRIPLET device that was used for the *in situ* measurements of [Chl *a*].

The pigment concentrations found using HPLC indicates a two-bloom structure as well, considering [Chl *a*]. At the peak of each of the blooms, however, different compositions of pigments were found. The light harvesting pigments Peridinin and Chl *b* were found in larger amounts in the first bloom than the second bloom. Peridinin is a biomarker for dinoflagellates, and dinoflagellates were indeed found to be dominant at that time, using microscopy. Chl *b* is a biomarker for chloro-, prasino- and euglenophytes, and as many of these taxa contain small cells, they were probably counted among the flagellates during the microscopy. During the second bloom, the light harvesting pigments Fucoxanthin and Chl *c*<sub>1</sub> and Chl *c*<sub>2</sub> had the highest concentration when excluding Chl *a*. These pigments together often indicate the presence of diatoms, and a dominance of diatoms was indeed found using microscopy.

The taxonomy of the counted samples reveals that the first observed bloom was dominated by dinoflagellates, at 53% of the total number of cells, followed by flagellates, at 32 % of the cell concentration found on the 15<sup>th</sup> of March. *Heterocapsa rotundata*, with a maximum concentration of 1734 cells mL<sup>-1</sup>, was the taxon found with the highest concentration in this first bloom. The second bloom was dominated by centric diatoms, at 73% of the cell concentration, followed by flagellates, at 20% of the cell concentration on the 1<sup>st</sup> of March. The taxon found to have the highest concentration during this bloom, at 2482 cells mL<sup>-1</sup> on

the 1<sup>st</sup> of April, was *Skeletonema costatum*. If all taxa belonging to the genus *Chaetoceros* were to be counted together, this would make up the second largest cell concentration, at 2045 cells mL<sup>-1</sup> on the 1<sup>st</sup> of April.

According to previous studies done in Trondheimsfjorden (Jensen and Sakshaug 1973; Sakshaug 1972) the spring bloom is usually dominated by diatoms. The second bloom observed is in accordance with these studies, but the first bloom is not, being dominated by dinoflagellates.

Both dinoflagellates and diatoms create a brownish colour when they are highly concentrated. This comes from the pigments Fucoxanthin (appears brown at high concentrations) from diatoms, and Peridinin (appears brick red at high concentrations) from dinoflagellates. Therefore, at high concentrations of these algae, one would expect a brownish ocean colour, not the greenish colour observed during the spring bloom at TBS. The major causes for this are, most probably, the absorbance of cDOM (appears green at low concentrations) and absorbance and scattering by TSM (appears grey-brown at high concentrations).

The covariation of cDOM and TSM was checked by dividing [cDOM] by the measure of the amount of TSM, which, when two outliers were removed, had a mean of 2.21 and a standard deviation of 0.85. The relatively low standard deviation indicates that the two variables covary to a degree. This co-variation is most likely due to cDOM and TSM having the same source, from river run-off.

By checking all possible combinations of variables, the best-fitting linear regression model to explain the Forel-Ule observations from IOPs was found to include [cDOM] and [TSM] as significant contributors ( $p = 0.0198$  and  $p = 0.0253$  respectively) and the interaction between these variables was also found to be a significant contributor ( $p = 0.0409$ ). The modelling process indicates that during the spring bloom time series, [Chl *a*] does not contribute significantly to the observed change in Forel-Ule number. When the data was normalised and then adjusted for the exhibited range of data, [TSM] contributes the most to changes in the colour, according to the model. [cDOM] and [TSM] are independent variables, having no causal link. However, their interaction indicates that they mainly originate from the same source. Therefore, any change in Forel-Ule number could be attributed to changes in the

[cDOM] and [TSM] contributed from river run-off, which is the most likely source of these substances in Trondheimsfjorden in spring (Sakshaug and Sneli 2000).

### Evaluating the Forel-Ule scale

Figure 19 from (Wernand 2011) shows the same relationship between the Secchi depth and the Forel-Ule number as I have found during this thesis (see Figure 11). The relationship is one of decreasing Secchi depth with increasing Forel-Ule number, following a power trend line. If all data points were found to fall exactly on the trend line, there would be no point in taking Fore-Ule measurements, as the Forel-Ule number could be calculated from the Secchi depth using the formula for the relationship between them. The total variation of all data points around the power trend line therefore indicates the additional information that can be obtained by using the Forel-Ule scale with the Secchi depth in comparison to just measuring Secchi depth.

Points on the inverse graph of Forel-Ule numbers that deviate from the trend of the Secchi depth during the spring bloom period are deviations from the trend in the same way as above. As Forel-Ule number indicates the spectral optical characteristics of the water, these deviations may indicate changes in this property of the water. Changes in the spectral optical characteristics of the water may indicate a change in the composition of IOPs in the water.

Deviations from the Secchi depth trend happens on the 11<sup>th</sup>, 15<sup>th</sup> and 29<sup>th</sup> of March, and on the 1<sup>st</sup> and 5<sup>th</sup> of April, with the Forel-Ule number being lower than expected from the trend in Secchi depth. These dates coincide with the blooms observed. To examine the difference closer, the FUNS factor was created by subtracting the Secchi depth from the inverted Forel-Ule number. This leaves the part of the Forel-Ule number that is not determined by the Secchi depth. The FUNS factor shows a similar two-bloom structure to the *in vitro* [Chl *a*] from HPLC, with the rise between the blooms possibly being a result of increased cDOM and TSM concentration (Figure 7, Figure 13). The FUNS factor seems to be to a greater extent decided by [Chl *a*] than is the Forel-Ule number. The FUNS factor could possibly be used as an indication of blooms in Case 2 waters. However, this was only done for a single bloom time data set, with Forel-Ule numbers ranging from 8 to 14, and only future research will show if this factor is indeed a useful one.

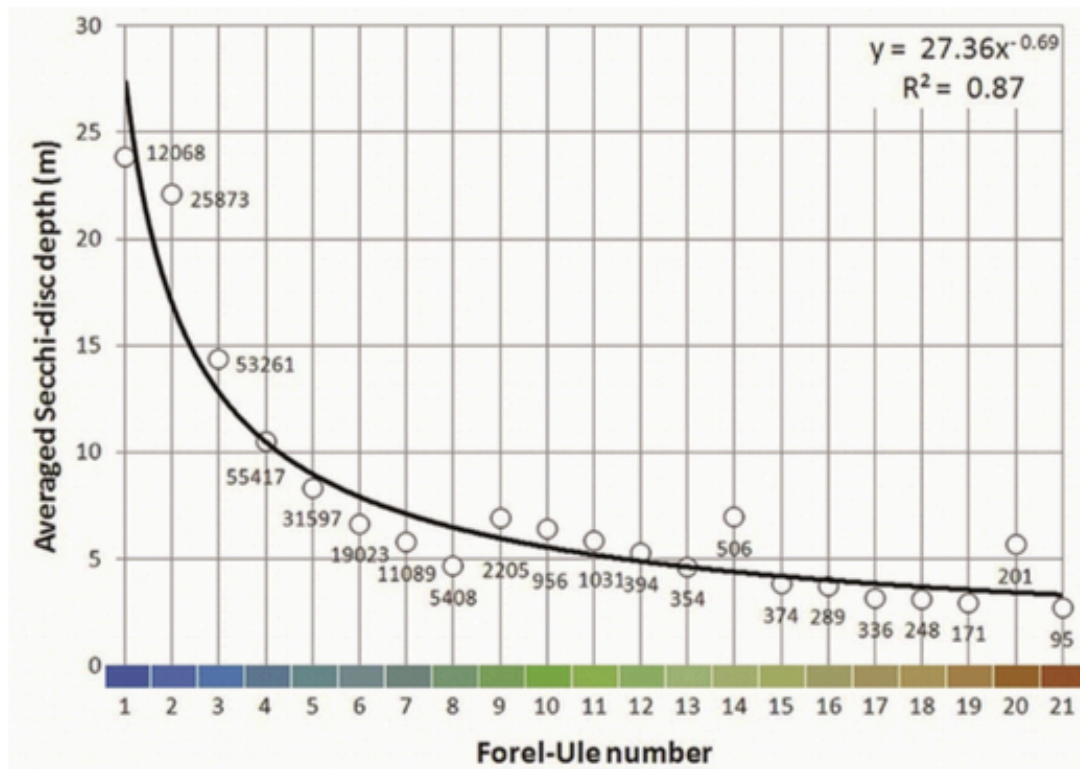


Figure 19: A review of Secchi depth measurements shown as a function of Forel-Ule number, with an exponential trendline. From: Wernand (2011)

Directly comparing Secchi depth and Forel-Ule number using inverse Forel-Ule numbers assumes a linear relationship between them. The Forel-Ule numbers measured during the spring bloom series are all between 8 and 14 (Figure 5), which is within the nearly linear part of the Secchi vs Forel-Ule graph (Figure 11, Figure 19). The assumption of a linear relationship is therefore reasonable.

The graphs of [Chl *a*] and total cell concentration shown as a function of the Forel-Ule number show no clear trend, but there is an indication of a possible linear upper limit. This upper limit seems to exist for both proxies of phytoplankton biomass within the most tested interval of Forel-Ule number 7 (FU7) to FU14, which is the green interval. This indicates that there may be a maximum [Chl *a*] and a maximum cell concentration possible for each Forel-Ule colour. It also indicates that there may exist a minimum Forel-Ule number given a certain [Chl *a*] or cell concentration has been found. As the most useful direction to be able to go would be from Forel-Ule number to [Chl *a*] or cell concentration, the connection found is not very useful. It shows that the [Chl *a*] may vary quite a lot for each Forel-Ule

number, and Forel-Ule number is therefore of little use in predicting phytoplankton biomass. These conclusions are only valid in the green interval of the Forel-Ule scale.

The similarity of the shape of the spectral attenuation coefficient for the water and the spectral attenuation of the corresponding Forel-Ule filter gives an indication that the Forel-Ule number together with the Secchi depth may be used to indicate the light climate in the water column. The Forel-Ule number would indicate the spectral optical characteristics of the water, while the Secchi depth would indicate the total water transparency. The shapes of the attenuation curves are quite similar but the curve of water  $K_d$  has a broader band of wavelengths around the blue-green wavelengths where little attenuation happens.

The attenuation coefficient  $K_d$  of the water can be calculated from the Secchi depth using Equation 2. The  $K_d$  calculated from the Secchi depth were generally in agreement with the spectroradiometer and irradiance sensor for the measurements at Froan, but not at Svalbard. For all the measurements done at Svalbard, the  $K_d$  calculated from Secchi depth was about 0.5 to 0.8  $m^{-1}$  lower than the values from spectroradiometer and irradiance sensor. The most probable reason for this is depth measurement errors in the measurements using the spectroradiometer and the irradiance sensor. These errors occurred because at Svalbard, the only depth measurements done were using length markers on the rope connected to the sensors. At Froan, a CTD was connected to the rig to ensure correct depth measurements. Another point of note is that the rope of Secchi disk was absorbing water and thus becoming thicker and approximately 7% shorter, and thus maybe affecting the Secchi depth measurements.

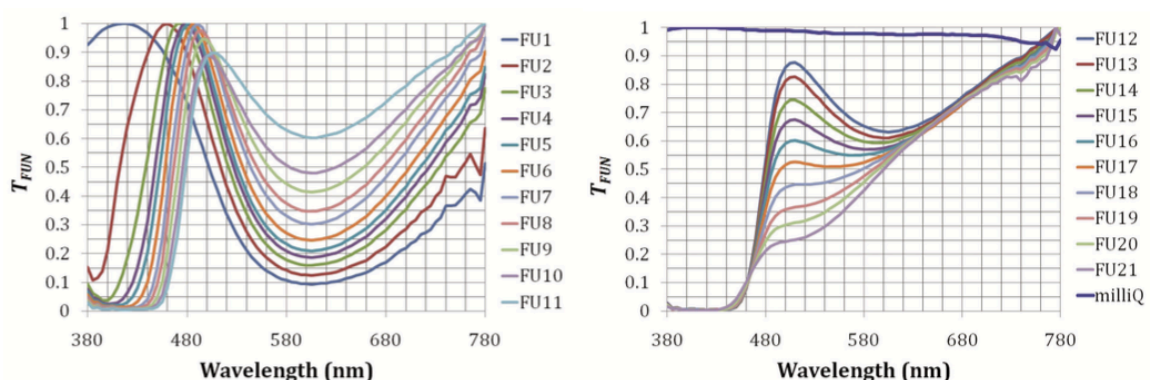


**Figure 20: The normalised transmission of the original solutions as devised by Forel and Ule. From Wernand (2011)**

The normalised light transmission spectra for the plastic Forel-Ule filters (Figure 16) show a similar shape to the ones from Wernand (2011) (Figure 20), which were for the original solutions of Forel and Ule (Forel 1890; Ule 1892). There are, however, some recurring peaks and troughs. These occur in the pattern of a peak at about 580 nm, a trough at about 618 nm, a peak at about 645 nm, and a trough at about 666 nm. As these are approximately the same for most filters, it is reasonable to suppose that they are a product of the plastic used to create the filters. The plastic filters seem to be close to the solutions, and that any “bumps” are not intended and can be considered artefacts. The transmission spectra and the attenuation spectra of the filters may be of use in translating between Forel-Ule number and a measurement of the spectral optical characteristics of the water. They could also aid in creating maps and comparing historical Forel-Ule data to modern data from spectroradiometer measurements.

The Secchi depth can be used to indicate the irradiance in the water column, and how far it penetrates. The Forel-Ule number can then indicate the spectral irradiance in the water column, assuming a thoroughly mixed upper layer. Together with day length, these measurements may indicate the light climate in the water column.

The pictures shown of the Secchi disk at half the Secchi depth highlight some of the problems when using the Forel-Ule method. At many points during the measurements done for this thesis, the current made measurement with the sun on the measurer’s back impossible, because the current would drag the Secchi disk under the boat or dock where the measurement was being done, rendering it invisible. Therefore, many measurements had to be conducted with the sun in the face of the measurer. It is then impossible to keep the water surface in shade, and light reflecting off the surface of the ocean can make measurement more difficult, as seen on the right in Figure 17. Wave action will also complicate both the Forel-Ule measurement, due to reflections from the waves, and the Secchi depth measurement due to unsure depth measurement. If the ocean is calm, however, a measurement with the sun in the face of the measurer can be easy, with the disk easily visible and uninterrupted by reflection as seen on the left in Figure 17.

### **Evaluation of the use of the Forel-Ule scale for citizen science**

To examine the results of the user test, it is important to be aware of the concepts of precision and accuracy. Precision is when the measurements fall within a short distance of each other

with a low standard deviation. Accuracy, however, is how close the measurements are to the actual value one is trying to measure, such as the bulls-eye in darts.

One could imagine a target for shooting practice. If all the shots fall within a small area, but that area is not the bulls-eye, the shooter has high precision, but low accuracy. If, however, the shots are spread out over a larger area, but the centre of that area includes the bulls-eye, the shooter has high accuracy, but low precision. The aim when shooting and when taking measurements is always to achieve both high precision and high accuracy.

The Forel-Ule measurements from the user test have low precision. The accuracy of the measurements is hard to determine, as human perception is involved, and it is difficult to set a standard. A possible standard could be the spectral attenuation,  $K_d(\lambda)$ , measured using a spectroradiometer, but this would require interpretation and translation into a Forel-Ule number, and this method is not developed enough to make this a good assumption. In addition, the spectral attenuation was not measured when the user test was conducted, so there is no possibility of comparison.

The Secchi depths from the user test have a relatively low standard deviation compared to the mean value at  $7.2 \pm 0.2$  m. This indicates that Secchi depth measurements taken by different people do not differ to a great degree. Forel-Ule measurements, however, showed a much higher variation, with low precision which is most likely caused by different colour perception in different people (Roaf 1927). This highlights the individual nature of colour perception, even when said perception is corrected for by asking each person to compare colours to find the closest match (Roaf 1927). An additional factor that might contribute to the variation in Forel-Ule measurements was that a front in the water was observed passing the measurement place, indicating that a change in water masses had taken place during the measurement time.

When taking Forel-Ule measurements, the human eye is the sensor in use. The range of the human eye is from 400 nm to 700 nm, with the highest sensitivity at 555 nm in daylight (Sakshaug et al. 2009b). All these values vary individually, and even in people with no colour-blindness, colour is seen and interpreted differently (Roaf 1927). The white balance used in a camera is akin to processes happening in the brain after observing colour (Sencar and Memon 2013).

Measurements using the Citclops app without a Secchi disk at half the Secchi depth show a large difference between the Forel-Ule numbers measured using the physical scale and the app, at  $4.2 \pm 2.0$ , indicating the low accuracy of the app measurements. The use of the app without a Secchi disk was due to a misunderstanding of the instructions, and as this app is intended for use as an app for citizen science, this misunderstanding could easily happen again. It appears that the app allows the user to make measurements without using a Secchi disk, and this would probably lead to such inaccuracies as found here. The Citclops app measurements when using a Secchi disk, as well as the Eye on Water measurements both with and without a Secchi disk, were closer to the physical Forel-Ule measurements than using the Citclops app without a Secchi disk. However, since these measurements were carried out few times ( $n=2$ ,  $n=4$  and  $n=4$  respectively, see Table 6), these results are not conclusive.

Crowdsourcing of scientific measurements could be a valuable resource if the results can be trusted. If everyone can become a hobby-scientist, it may also aid in spreading awareness and new information, keeping people primed for scientific-based knowledge. In addition, with the use of the Internet, everyone can see their measurements as a part of a larger whole and feel like a part of a scientifically active community. More data points gathered by the community will also yield a greater spatial and temporal resolution of datasets, which may help scientists who can compare these to other data types, for example remote sensing imagery. On the other hand, it is doubtful how much weight one could give to crowd sourced data. As seen from the user test in this thesis, as well as the tests of the apps, the data will likely have low precision and accuracy. The instructions in an app may be difficult to follow or easy to misinterpret. In addition, if the smartphone apps have not been written to keep white balance constant, this could be a confounding factor for the accuracy of the measurements.



## Conclusions and future perspectives

During the spring bloom at TBS, the modern methods of measuring AOPs and IOPs, using a spectroradiometer, *in situ* fluorescence- and backscattering, HPLC and light microscopy, gave a much more detailed picture than could be gained from Forel-Ule measurements. [Chl *a*], measured both *in situ* and *in vitro*, showed a two phytoplankton blooms during the measurement period, and phytoplankton pigment concentrations and light microscope taxonomy data confirmed this. In addition, pigment concentrations and microscopy revealed that the two observed blooms were of different taxonomic composition, the first one dominated by dinoflagellates, and the second one dominated by diatoms. By use of linear regression, it was found that [Chl *a*] had no significant effect on the Forel-Ule number, but that [cDOM] and [TSM] did. Further research is needed to show the effect of low concentrations of cDOM and TSM and combinations of these on ocean colour. It was found that the difference between the inverse Forel-Ule number and the Secchi depth, termed the FUNS factor, showed the two-peak pattern found in [Chl *a*], which could indicate that the part of the Forel-Ule number which is not determined by the Secchi depth is to a greater extent decided by [Chl *a*] than is the Forel-Ule number itself. This, however, is by no means a certainty, as this was only done for one spring bloom data set, and more research would be needed to see if this relationship is indeed a useful one.

The usefulness of the Forel-Ule scale as an addition to the Secchi depth is dependent upon how much it might vary from the relationship found between Forel-Ule number and Secchi depth in this thesis and in Wernand (2011). The Forel-Ule scale might be a good measure of the algal concentration in Case 1 waters, but not necessarily the more optically complex Case 2 waters. The concentrations of TSM and cDOM seem to be masking the effect of algal biomass on the Forel-Ule number in the Trondheimsfjord, while the only significant optical components of Case 1 waters are the water itself and phytoplankton. The user test conducted in this thesis showed a low precision of Forel-Ule measurements conducted by different people. This, and the differences between measurements done using smartphone apps and the physical Forel-Ule scale, indicates that using the Forel-Ule scale for citizen science has its weaknesses. More research is needed to prove that the Eye on Water smartphone app can consistently give the same results as a physical scale. I would recommend not allowing users to submit results found without the use of a Secchi disk, if the Eye on Water app is like the Citclops app. As the Secchi depth was found to have a high precision in the user test, this

might be a better use of citizen science, to ensure that the measurements would be useful to scientists.

The Forel-Ule scale would be useful in connecting measurements of ocean colour in the past with ocean colour of today, though more research is needed to be able to translate spectroradiometer data collected today to Forel-Ule number for historical data comparisons. In fields where categories of ocean colour are useful, such as remote sensing, oceanography and modelling, where large-scale maps of ocean colour and corresponding phytoplankton biomass would be made, Forel-Ule can be a powerful tool for visualising and categorizing ocean colour.

## Bibliography

- Brunet C, Johnsen G, Lavaud J, Roy S (2011) Pigments and photoacclimation processes. In: Roy S, Llewellyn CA, Egeland ES, Johnsen G (eds) *Phytoplankton Pigments: Characterization, Chemotaxonomy and Applications in Oceanography*. Cambridge University Press
- Cadée GC (1996) Michael Faraday and his “Secchi disks” *Archives of Natural History* 23:291-294
- Citclops (2014) Citclops. <http://citclops.eu/>. Accessed 15.05. 2017
- Cotter CH, Morgan JR, Bardach JE Pacific Ocean. *Encyclopædia Britannica, inc.* <https://global.britannica.com/place/Pacific-Ocean>. Accessed 05.05 2017
- Edler L, Elbrächter M (2010) The Utermöhl method for quantitative phytoplankton analysis. UNESCO, Paris
- Falkowski PG, Raven JA (2007) *Aquatic Photosynthesis* (Second Edition). STU - Student edition edn. Princeton University Press,
- Forel FA (1890) Une nouvelle forme de la gamme de couleur pour l'étude de l'eau des lacs *Archives des sciences physiques et naturelles/Societe de physique et d'histoire naturelle de geneve* 6:25
- Foster DH, Nascimento SM, Craven B, Linnell KJ, Cornelissen FW, Brenner E (1997) Four issues concerning colour constancy and relational colour constancy *Vision research* 37:1341-1345
- Gegenfurtner KR, Sharpe LT (2001) *Color vision: From genes to perception*. Cambridge University Press,
- Hegseth EN, Tverberg V (2013) Effect of Atlantic water inflow on timing of the phytoplankton spring bloom in a high Arctic fjord (Kongsfjorden, Svalbard) *J Marine Syst* 113:94-105
- Hubel DH (1963) *The visual cortex of the brain*
- Jeffrey SW, Simon WW, Zapata M (2011) Microalgal classes and their signature pigments. In: Roy S, Llewellyn CA, Egeland ES, Johnsen G (eds) *Phytoplankton pigments: Characterization, Chemotaxonomy and Applications in Oceanography*. Cambridge University Press
- Jensen A, Sakshaug E (1973) Studies on the phytoplankton ecology of the trondheimsfjord. II. Chloroplast pigments in relation to abundance and physiological state of the phytoplankton *J Exp Mar Biol Ecol* 11:137-155

- Jerlov NG (1976) Marine optics vol 14. Elsevier
- Johnsen G, Moline MA, Petterson LH, Pinckney J, Pozdnyakov DV, Egeland ES, Schofield OM (2011) Optical monitoring of phytoplankton bloom pigment signatures. In: Roy S, Llewellyn CA, Egeland ES, Johnsen G (eds) Phytoplankton Pigments: Characterization, Chemotaxonomy and Applications in Oceanography. Cambridge University Press
- Johnsen G, Sakshaug E (2007) Biooptical characteristics of PSII and PSI in 33 species (13 pigment groups) of marine phytoplankton, and the relevance for pulse - amplitude - modulated and fast - repetition - rate fluorometry *Journal of Phycology* 43:1236-1251
- Johnsen G, Volent Z, Sakshaug E, Sigernes F, Petterson LH (2009) Remote sensing in the Barents Sea. In: Sakshaug E, Johnsen G, Kovacs KM (eds) *Ecosystem Barents Sea*. Tapir Academic Press, Trondheim, Norway
- Karleskint G, Turner R, Small J (2012) *Introduction to marine biology*. Cengage Learning,
- Karlson B, Cusack C, Bresnan E (2010) *Microscopic and Molecular Methods for Quantitative Phytoplankton Analysis*. UNESCO
- Kedra M et al. (2015) Status and trends in the structure of Arctic benthic food webs *Polar Res* 34
- Kirk JT (1994) *Light and photosynthesis in aquatic ecosystems*. Cambridge university press,
- Kon-Tiki2 (2015) Kon - Tiki 2. Accessed 15.05. 2017
- MARIS, Citclops (2016) EyeOnWater. <http://www.eyeonwater.org/>. Accessed 15.05 2017
- Martin VY (2017) Citizen Science as a Means for Increasing Public Engagement in Science: Presumption or Possibility? *Science Communication* 39:142-168
- Mason P, Reading B Implementation plan for the global observing systems for climate in support of the UNFCCC. In: *Proceedings of the 21st international conference on interactive information processing systems for meteorology, oceanography, and hydrology, 2005*.
- Preisendorfer RW (1976) *Hydrologic Optics. Volume 5. Properties*. Honolulu: US Dept. of Commerce, National Oceanic and Atmospheric Administration, Environmental Research Laboratories, Pacific Marine Environmental Laboratory,
- Raman CV (1922) On the molecular scattering of light in water and the colour of the sea *Proceedings of the Royal Society of London Series A, Containing Papers of a Mathematical and Physical Character* 101:64-80

- Roaf H (1927) THE RELATION OF WAVE - LENGTH AND LIGHT INTENSITY TO COLOUR DISCRIMINATION IN NORMAL AND HYPOCHROMATIC (COLOUR BLIND) INDIVIDUALS Quarterly Journal of Experimental Physiology 16:379-392
- Rodriguez F, Chauton M, Johnsen G, Andresen K, Olsen LM, Zapata M (2006) Photoacclimation in phytoplankton: implications for biomass estimates, pigment functionality and chemotaxonomy Mar Biol 148:963-971
- Roy S, Llewellyn CA, Egeland ES, Johnsen G (2011) Phytoplankton pigments: characterization, chemotaxonomy and applications in oceanography. Cambridge University Press
- Sakshaug E (1972) Phytoplankton Investigations in Trondheimsfjord, 1963-1966 Det Kongelige Norske Vitenskabers Selskab Skrifter 1:56
- Sakshaug E, Johnsen G, Kristiansen S, Quillfeldt Cv, Rey F, Slagstad D, Thingstad F (2009a) Phytoplankton and primary production. In: Sakshaug E, Johnsen G, Kovacs KM (eds) Ecosystem Barents Sea. Tapir Academic Press, Trondheim, Norway
- Sakshaug E, Johnsen G, Volent Z (2009b) Light. In: Sakshaug E, Johnsen GH, Kovacs KM (eds) Ecosystem Barents Sea. Tapir Academic Press, Trondheim, Norway
- Sakshaug E, Sneli J-A (2000) Trondheimsfjorden. Tapir forlag, Trondheim
- Sathyendranath S (2000) Reports of the International Ocean-Colour Coordinating Group IOCCG, Dartmouth, Canada 3:140
- Sencar HT, Memon N (2013) Digital image forensics Counter-Forensics: Attacking Image Forensics:327-366
- Silvertown J (2009) A new dawn for citizen science Trends in Ecology & Evolution 24:467-471
- Simon M, Alldredge AL, Azam F (1990) Bacterial carbon dynamics on marine snow Mar Ecol Prog Ser:205-211
- Suggett DJ, Prášil O, Borowitzka MA (2010) Chlorophyll a fluorescence in aquatic sciences: methods and applications. Springer
- Sverdrup H (1953) On conditions for the vernal blooming of phytoplankton Journal du Conseil 18:287-295
- Ule W (1892) Die bestimmung der Wasserfarbe in den Seen Kleinere Mittheilungen Dr A Petermanns Mittheilungen aus Justus Perthes geographischer Anstalt:70-71
- Utermöhl H (1958) Zur Vervollkommnung der quantitativen Phytoplankton-Methodik Der Internationalen Vereinigung für Limnologie:1-38

- Valle KC (2014) Photoacclimation mechanisms and light responses in marine micro- and macroalgae. NTNU
- Watson J, Zielinski O (2013) Subsea optics and imaging. Elsevier,
- Wernand MR (2011) Poseidon's paintbox: Historical archives of ocean colour in global-change perspective. University of Utrecht

# Appendix 1

## Citclops app instructions taken from citclops.eu

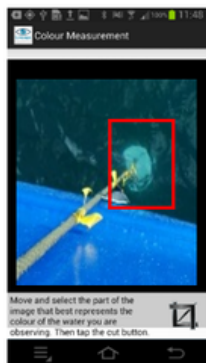
Select Colour measurement Icon



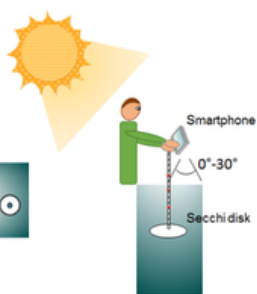
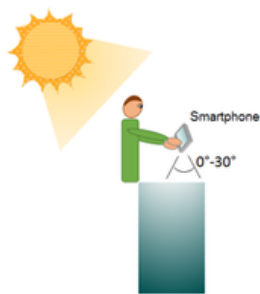
Take a picture with the sun on your back, and part of the image



If you have a Secchi disk select it on the image



Compare the colour of the water with the colour bars.



## EyeOnWater instructions taken from the application

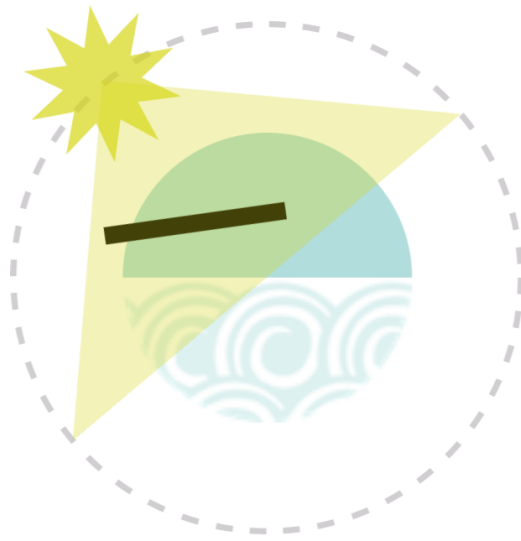
### Introduction movie



Hold phone horizontally  
to the water surface..

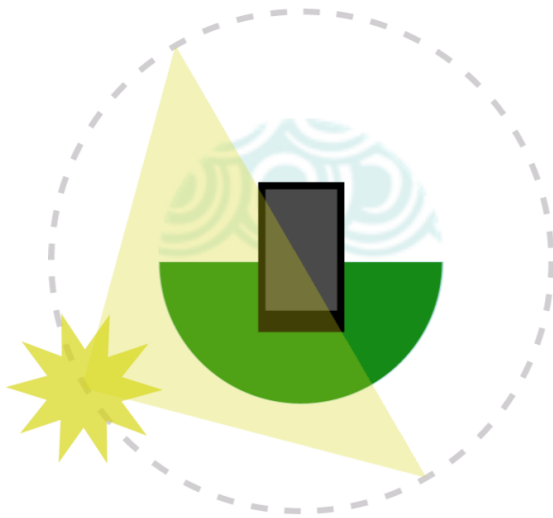
**Skip intro**





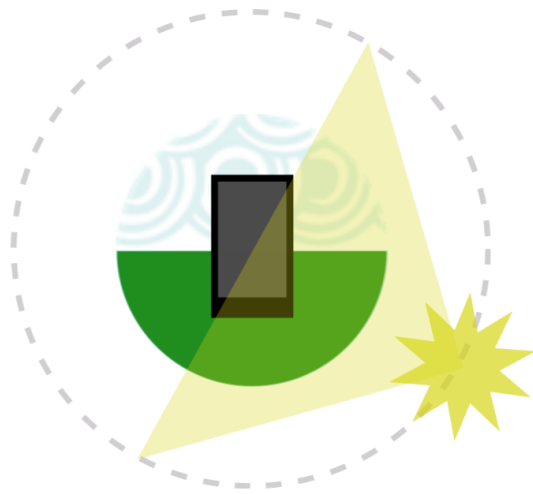
Place yourself with the  
sun on your back..

**Skip intro**



Shining over your left..

**Skip intro**



Or your right shoulder..

**Skip intro**

Home page of the app



EyeOnWater.org



## COLOUR

An App to classify fresh  
and saline natural waters  
on their colour.

Point your camera to the  
water surface

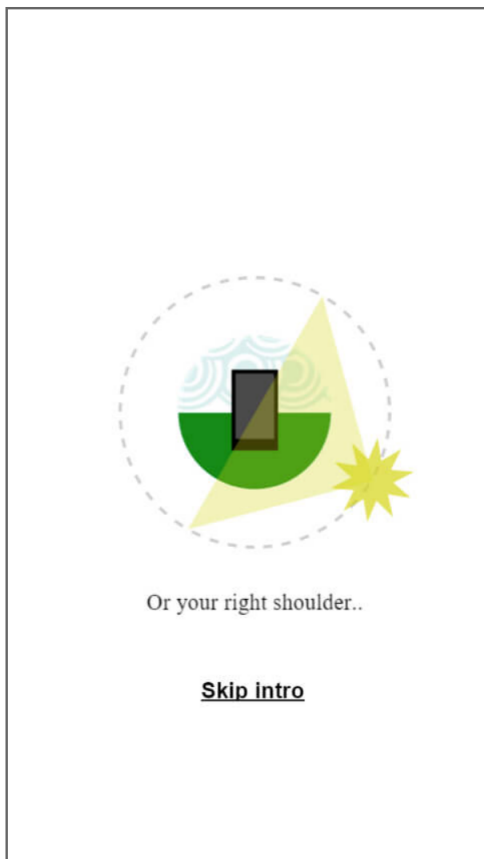
**GET STARTED**

How to use



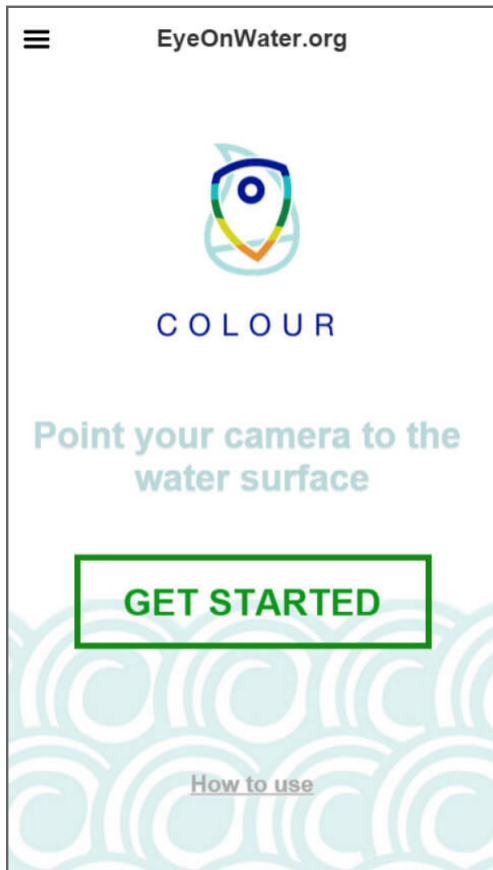
### Step 1. View the introduction movie

The movie shows you how to position yourself: With your back against the sun pointing over your shoulder. This provides the best measurements.



### Step 2. The app homepage

Open the menu to find additional information and switch the intro 'off' if you do not want to see this every time you open the app.



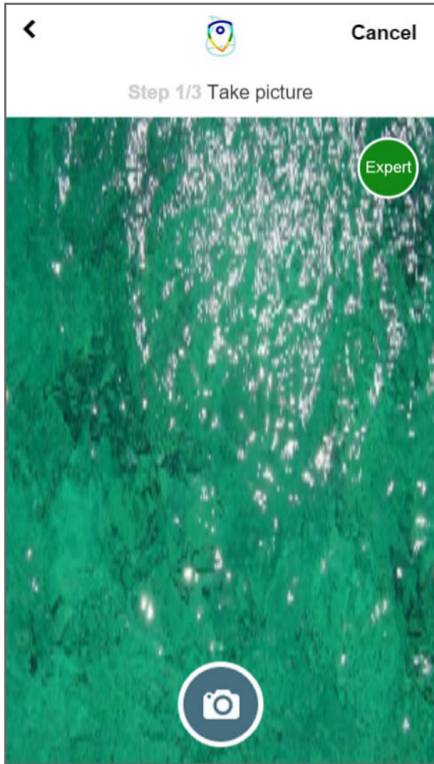
**Step 3. Get started:**

Take your colour Measurement (Main Screen)

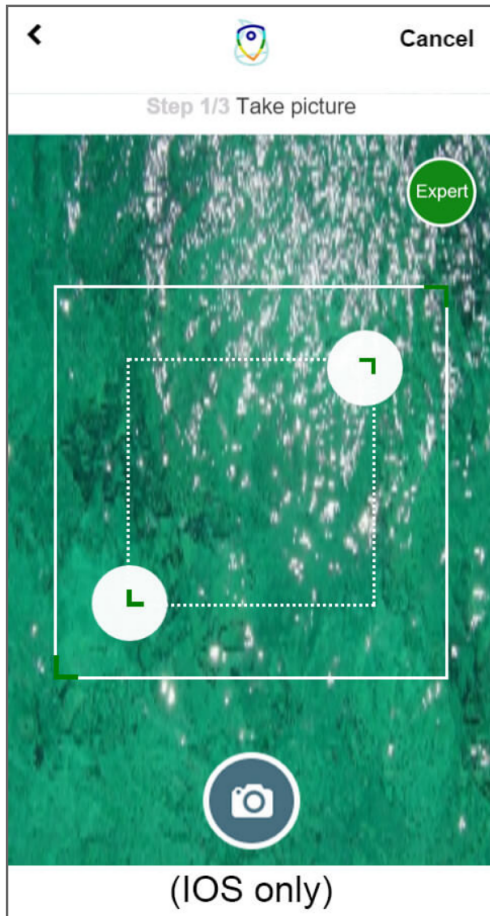
#### Step 4. Take a picture

Of the water with the sun on your back, over your left or right shoulder. The angle of the camera with respect to the water surface should be less than 30, otherwise the lens will not open. If it is cloudy and you do not see the sun, do not worry and just take a picture. If you have a Secchi disk, make sure it appears on the picture.









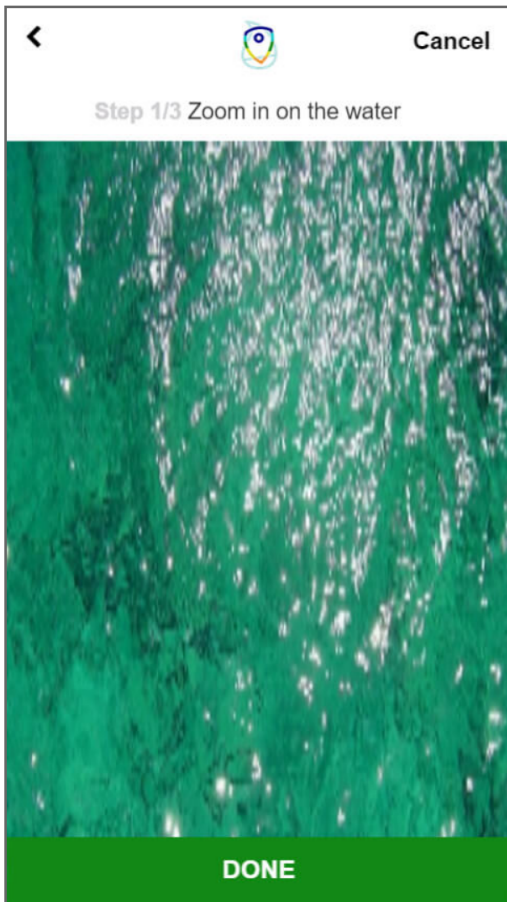
### Step 5. (Android only)

Look at the water on the image and zoom/pan to the part of the picture that best represents the colour of the water as you observe it without foam or sun reflection. If you have a Secchi disk (at  $\frac{1}{2}$  SDD), make sure it appears on the picture and you select that part. Do not wear sunglasses for this.

Then, tap the "done" button.



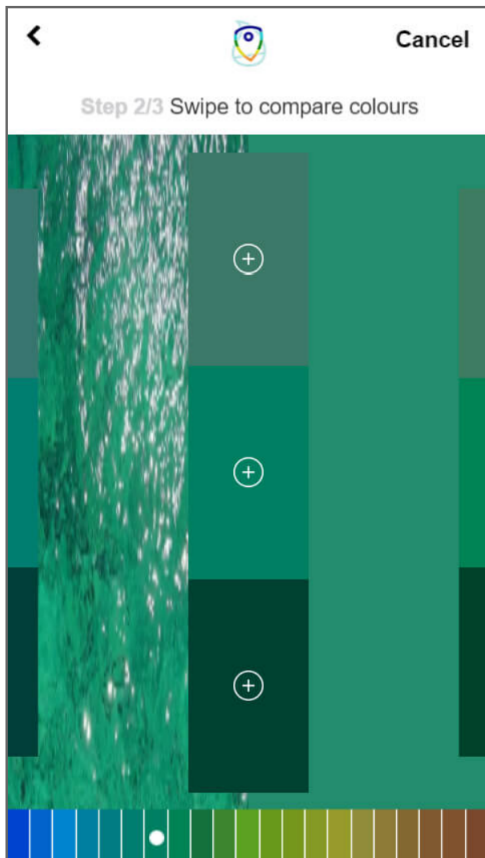
## How to use the app



### Step 6.

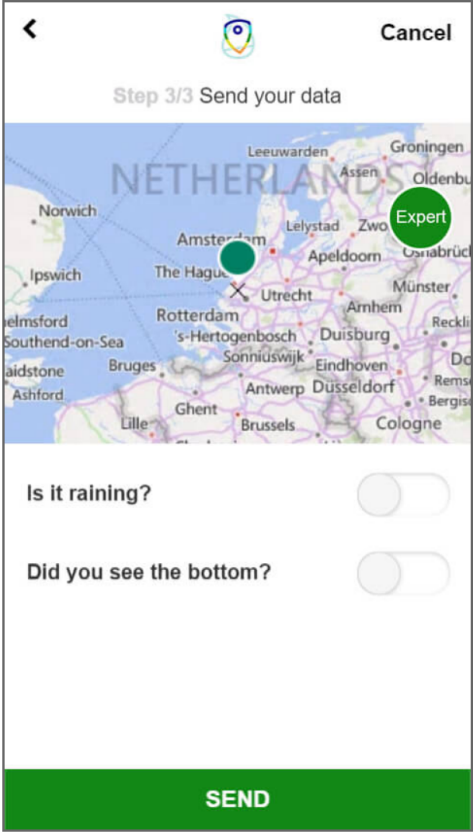
Compare the coloured bars with either the colour of the water you are observing or, if easier, with the colour of the picture you just cut. The right part of the screen already helps you with the “main” colour in the image. If you have a Secchi disk compare the coloured bars with the colour of the water above it (at  $\frac{1}{2}$  SDD).

Select one of the bars (3 colour tones each) that matches the colour of the water you are observing (Swipe the bar to see all the options). Then tap the colour bar (the + icon).



## Step 7.

Answer 2 simple questions



The screenshot shows a mobile application interface. At the top, there is a back arrow, a logo, and a 'Cancel' button. Below this, the text 'Step 3/3 Send your data' is displayed. The main area features a map of the Netherlands with several green circular markers. One marker is labeled 'Expert'. Below the map, there are two questions with toggle switches: 'Is it raining?' and 'Did you see the bottom?'. At the bottom of the screen, there is a prominent green button labeled 'SEND'.

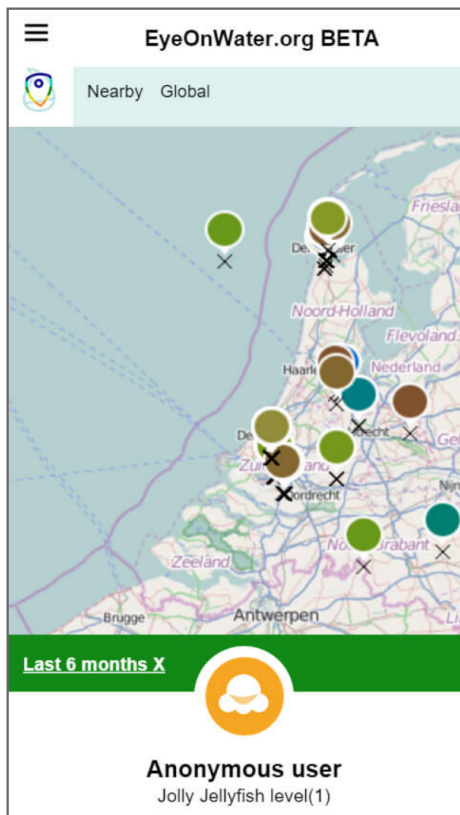
## Step 8.

Click Send

## Step 9. EyeonWater website

Go to the EyeonWater website to view all your own and other measurements. In order to view all your own images do not forget to register yourself first and then link your

mobile device to your account. After that you get a more personal experience and all your measurements are really identified as yours.



## Step 10. Survey

Answer survey questions via the website [www.citclops.eu](http://www.citclops.eu) (optional)

## Appendix 2

### Summary of final model using [cDOM] and Beta(700) as predictor variables

Call:

```
lm(formula = FU..physical.scale. ~ mean.cdom * mean.beta)
```

Residuals:

```
      1      2      3      4      5      6      7
-0.98212  0.53422  0.87209  0.19417 -0.36703 -0.65518  0.41887
      8
-0.01502
```

Coefficients:

	Estimate	Std. Error	t value	Pr(> t )
(Intercept)	0.2023	2.5344	0.080	0.9402
mean.cdom	10.0373	2.6702	3.759	0.0198 *
mean.beta	9.6794	2.7810	3.481	0.0253 *
mean.cdom:mean.beta	-7.4634	2.5069	-2.977	0.0409 *

---

Signif. codes: 0 '\*\*\*' 0.001 '\*\*' 0.01 '\*' 0.05 '.' 0.1 ' ' 1

Residual standard error: 0.8348 on 4 degrees of freedom

Multiple R-squared: 0.8963, Adjusted R-squared: 0.8185

F-statistic: 11.52 on 3 and 4 DF, p-value: 0.01946

### Summary of model using only [Chl $a$ ] as a predictor variable

Call:

```
lm(formula = FU..physical.scale. ~ CHL.ave)
```

Residuals:

```
      Min      1Q  Median      3Q      Max
-3.7633 -0.3909  0.5598  1.0093  2.2573
```

Coefficients:

	Estimate	Std. Error	t value	Pr(> t )
(Intercept)	11.49127	1.87351	6.134	0.000859 ***
CHL.ave	0.06726	0.30127	0.223	0.830757

---

Signif. codes: 0 '\*\*\*' 0.001 '\*\*' 0.01 '\*' 0.05 '.' 0.1 ' ' 1

Residual standard error: 2.108 on 6 degrees of freedom

Multiple R-squared: 0.008237, Adjusted R-squared: -0.1571

F-statistic: 0.04983 on 1 and 6 DF, p-value: 0.8308